Stockholm University

Edge Modes of $\mathbb{Z}_n$ Symmetric Chains

Licentiate Thesis in Theoretical Physics

Iman Mahyaeh

Akademisk avhandling för avläggande av licentiatexamen vid Stockholms universitet, Fysikum

January 22, 2018

Abstract

In this Licentiate Thesis we will study the topological phases of $\mathbb{Z}_2$ and $\mathbb{Z}_3$ symmetric chains. We will present the Kitaev chain, a $\mathbb{Z}_2$ symmetric model of spinless fermions, and obtain all the eigenstates of the model with an open boundary condition which hosts Majorana zero modes in the topological phase. We will also present zero modes of the Kitaev chain with phase gradient in the pairing term and longer range couplings. This model could host Majorana zero modes as well as 'one-sided' zero energy fermionic state. We will study the role of interactions on the topological phase by considering a special model for which one can obtain the ground states exactly. Similarly, for the $\mathbb{Z}_3$ case, we will present a 3-state clock model as well as a solvable model for which the ground states are obtained exactly. We will briefly address the presence of edge modes in these models as well.

Acknowledgements

First of all I should thank for all of my parents' and grandparents' supports in my life. They have provided all the best for me and I am so fortunate to have them besides myself.

I am grateful to Eddy. He is not only an excellent supervisor, but also a very good friend. I have learned quite a lot from him and try to learn more in future as well. My time with him would be an unforgettable nice memory.

I would like to thank my friends with whom I share an office. First of all Christian who taught me a lot about physics. We always have very fruitful discussions. Babak was always trying to change me to be a mathematician, to be *rigorous*. As you see he was unsuccessful, and I am still, and hopefully will be, in the physics community. We have had many nice time and quite a lot of fun. And Axel, with a never disappearing smile on his face, is always enthusiast about physics, which makes the discussions with him really pleasant.

I am also grateful my very best freinds, to Mahdi, Fariborz and their families with whom I always have nice time.

I am also grateful to all of my friends in the group, Hans, Supriya, Jonas L., Emil, Sören, Yaron, Thomas, Emma, Sree, Ole, Jonas K., Irina, Pil, Johan and Flore, with whom I had a very nice time and very fruitful discussions.

Contents

1

Introduction

Everybody in the physics community has probably heard of the 2016 Nobel prize in Physics which was about Topological Phases of Matter [1,2], the general concept in this licentiate. The Nobel committee in Physics has prepared two very nice intoductory articles, namely *popular information* [3] as well as *advanced information* [4], which we would recommend. Nevertheless, we will give a very brief introduction to the subject as well as the outline of this licentiate.

One of the goals of condensed matter theory is classifying phases of matter. Let us look at the usual way of classification, namely **Symmetry Breaking**. A typical example are the solid and liquid-gas phases and the phase transition between them. The Hamiltonian for this system, say water, has a kinetic as well as a potential term, all of which are translational invariant, so the full Hamiltonian is as well. One could ask: Does the ground state inherit the translational symmetry? In the liquid-gas phase the ground state is still translational invariant, however, in the solid phase the symmetry is broken to a subgroup of translation which is a discrete group. Put in another way, the wavefunction of a solid is only invariant if you translate everything with a vector of the underlying Bravais' lattice. Therefore the symmetries of the solid and liquid-gas phases are different and this helps us to distinguish between them.

There are other phases or phase transitions, however, which can not be classified by symmetry or symmetry breaking. One example is the Kosterlitz-Thouless transition which occurs in the classical XY model in 2 dimensions [4]. From numerics people had found that the magnetic susceptibility diverges at finite temperature [5], which is a strong signature of a phase transition. However, the Mermin-Wagner theorem excludes an ordered phase in 2 dimensions for a model with continuous symmetry [6–8], in this case $O(2)$. This paradox can be solved by taking into account vortices which could appear in the model. Each vortex is characterized by a winding number, "*the topological number*". At high temperatures the vortices are free to move in the system. On the

other hand for low temperatures vortices with opposite winding number bind together and form a pair. Hence there is indeed a phase transition for the vortices at finite temperature, although there is no symmetry breaking in the system.

An other example is the Integer Quantum Hall Effect(IQHE) [9]. If one measures the transverse resistance of a two dimensional electron gas subjected to a strong perpendicular magnetic field, one will see plateaus as a function of magnetic field. Each plateau is characterized by an integer number, n, and the resistance is $\rho = \frac{1}{n}\frac{h}{e^2}$ on the plateau, where h is the Planck constant and e is the electron charge. One can not describe these plateaus (phases) nor the transitions between them in terms of symmetry breaking. The plateaus are described by a topological invariant which is the Chern number of the occupied bands(the so-called TKNN invariant) [10].

These are examples of **Topological Phase Transitions**. In this licentiate we will also study models which have topological phases. We will present these models and characterize their phases.

In chapter 2 we will present the Transverse Field Ising model(TFIM) and study it in two limiting cases in both spin and fermionic languages. We will show that in the spin representation, the model has ordered and disordered phases which correspond to the topological and trivial phases respectively in the fermionic language. The fermionic representation of the model, the Kitaev chain, hosts Majorana zero modes(MZMs) in the topological phase [11], some signatures of existence of which have been seen in recent experiments [12–15]. As an application of MZMs we can mention their potential usage in quantum computation by taking advantage of their non-abelian statistics [16–18].

The Kitaev model is a non-interacting model of spinless fermions and hence solvable for a closed chain using Fourier and Bogoliubov transformations. One should notice that, however, MZMs appear in an **open chain** for which one does not have a good quantum number like momentum in the closed chain. This makes solving the problem harder. Nevertheless the model has been solved in two special cases previously. We have solved the general problem and obtained all the eigenvalues and eigenvectors and paid special attention to characterize the MZMs wavefunctions. We have also studied the model with next nearest hopping and superconductivity pairing which for some specific cases shows two MZMs, namely one localized Dirac fermion, on only one side of an open chain.

Having solved the non-interacting model, a natural question would be to consider the role of interaction and see how much of the physics will survive by adding it to the model. In chapter 3, we address this question by looking at a specific interacting model which is solvable, in the sense that one can write the ground states' wavefunction analytically. We will briefly discuss the notations of strong and weak zero modes in this context as well.

In chapter 3, we will also present a 3-state clock model, a generalization of the TFIM which has $\mathbb{Z}_3$ symmetry. This model has not been solved except for

the integrable lines, but it has been conjectured that it hosts **Parafermionic** zero modes which are generalization of MZMs. We will also present a new $\mathbb{Z}_3$ symmetric model for which we found exact ground states analytically. This generalization is not only a theoretical and conceptual interest, but is also required for the purpose of topological quantum computation. One can not make all the quantum gates using MZMs and their non-abelian statistics and ought to use a richer set of building blocks [17]. One proposal is using parafermion zero modes [19].

In chapter 4, we will conclude and discuss the outlook of our projects.

2

From The Transverse Field Ising Model To The Kitaev Chain

2.1 Introduction

Exactly solvable models in statistical mechanics are quite fruitful. The XY model [20] and Transverse Field Ising Model(TFIM) [21] are two insightful examples of them. The following general Hamiltonian contains both models in specific limits as will be shown later,

$$H = -\sum_{j=1}^{L-1} \left(J_x \sigma_j^x \sigma_{j+1}^x + J_y \sigma_j^y \sigma_{j+1}^y \right) - h \sum_{j=1}^{L} \sigma_j^z \ , \tag{2.1}$$

in which $\sigma_j^\alpha (\alpha = x, y, z)$ are Pauli matrices, J_x,J_y and h are real coupling constants and L is total number of sites. Note that the Hamiltonian has open boundary conditions(OBC).

One can look at the model differently using the Jordan-Wigner(JW) transformation,

$$\sigma_j^x = \left[\prod_{k=1}^{j-1} (1 - 2n_k) \right] (c_j + c_j^\dagger) \ , \tag{2.2}$$

$$\sigma_j^y = \left[\prod_{k=1}^{j-1} (1 - 2n_k) \right] \frac{(c_j - c_j^\dagger)}{i} \ , \tag{2.3}$$

$$\sigma_j^z = 1 - 2n_j \ , \tag{2.4}$$

in which c_j is a spinless fermion annihilation operator, $n_j = c_j^\dagger c_j$ and they satisfy the usual fermionic algebra,

$$\{c_i, c_j^\dagger\} = \delta_{ij} \ . \tag{2.5}$$

We map the model to a non-interacting model of spinless fermions by JW transformation,

$$H = \frac{1}{2}\sum_{j=1}^{L-1}(c_j^\dagger c_{j+1} + \Delta c_j^\dagger c_{j+1}^\dagger + h.c.) - \mu\sum_{j=1}^{L}(c_j^\dagger c_j - \frac{1}{2}) \ , \tag{2.6}$$

in which we defined $\Delta = 2(J_y - J_x)$, $\mu = -2h$ and we set $J_x + J_y = -\frac{1}{2}$. In the fermionic language the model is quadratic, thus solvable.

There are two rather different viewpoints towards the model. In one viewpoint one can consider spins as the basic constituents of the system, say looking at magnetic system, and appreciate the spinless fermion representation just as a neat trick to solve the model. In this context, the model has two phases, ordered and disordered. In the ordered phase we have symmetry breaking and the system shows a magnetic behavior. On the other hand in the disordered phase spins are oriented in random directions.

In another way of thinking, one can totally forget about the spin model and ask what would be the phases of the model if spinless fermions were the real degrees of freedom? If the model in the spin language has two phases, what are those in the fermionic one? Is there any order parameter?

It turns out that in the fermionic language the model has trivial and topological phases which correspond to disordered and ordered phases in the spin language respectively. As you will see there is a **topological number** instead of order parameter which differs in these two phases. A crucial feature of the topological phase is the presence of Majorana zero modes, which can be thought of as "half" of a fermion.

To show these features, first we will discuss symmetries of the model. After that we will look at two limiting cases of the model in both spin and fermionic languages to study the different phases. We will close this chapter by briefly presenting our results about the model with general coupling constants and its variations.

2.2 Symmetries

We start by explaining a nice symmetry of the model, namely particle-hole symmetry. The claim is that H in Eq.2.1 and $-H$ have the same spectrum. Consider $-H$,

$$-H = \sum_{j=1}^{L-1}\left(J_x\sigma_j^x\sigma_{j+1}^x + J_y\sigma_j^y\sigma_{j+1}^y\right) + h\sum_{j=1}^{L}\sigma_j^z \ . \tag{2.7}$$

The spectrum of any Hamiltonian only depends on the algebra of operators in it. Hence one can consider another representation of the $SU(2)$ algebra [11],

$$\begin{aligned} \sigma^x_{2n-1} &\to -\sigma^x_{2n-1}, & \sigma^x_{2n} &\to \sigma^x_{2n}, \\ \sigma^y_{2n-1} &\to \sigma^y_{2n-1}, & \sigma^y_{2n} &\to -\sigma^y_{2n}, \\ \sigma^z_{2n-1} &\to -\sigma^z_{2n-1}, & \sigma^z_{2n} &\to -\sigma^z_{2n} \ . \end{aligned} \tag{2.8}$$

With this new representation we would get H back. Therefore the spectrum of H and $-H$ are the same. In the fermionic picture this is known as particle-hole symmetry.

Another symmetry of the model is the $\mathbb{Z}_2$ symmetry. One can define a parity operator, $P = \prod_{k=1}^{L} \sigma^z_k = \prod_{k=1}^{L} (-1)^{n_k}$, which has two eigenvalues, ± 1, since $P^2 = \mathbb{1}$ (the identity operator) and commutes with Hamiltonian, $[H, P] = 0$. In the ordered/topological phase of the model, one gets two ground states with different parity, however, in the disordered/trivial phase the ground state is unique and belongs to one parity sector.

Now we consider two special cases of the model, the XY model and the TFIM.

2.3 The XY Model

The XY model corresponds to $h = 0$. Using JW transformation Lieb et al [20] mapped the model to a free fermion model which is called a p-wave superconductor in the modern terminology. Except for the fine-tuning point $J_x = J_y$ for which one gets a gapless cosine band, the spectrum is gapped and shows magnetic behavior. We can understand this intuitively. First, note that in this case one can always assume that $J_x, J_y > 0$. If these couplings are not positive, we perform a canonical transformation. To see this we look at the following example,

$$H_{XY} = \sum_{j=1}^{L-1} -|J_x| \sigma^x_j \sigma^x_{j+1} + |J_y| \sigma^y_j \sigma^y_{j+1} \ . \tag{2.9}$$

Now one can transform Pauli matrices as follows,

$$\begin{aligned} \sigma^x_{2n-1} &\to \sigma^x_{2n-1}, & \sigma^x_{2n} &\to \sigma^x_{2n}, \\ \sigma^y_{2n-1} &\to -\sigma^y_{2n-1}, & \sigma^y_{2n} &\to \sigma^y_{2n}, \\ \sigma^z_{2n-1} &\to -\sigma^z_{2n-1}, & \sigma^z_{2n} &\to \sigma^z_{2n} \ . \end{aligned} \tag{2.10}$$

Performing this transformation would give the following Hamiltonian,

$$H_{XY} = -\sum_{j=1}^{L-1} \left(|J_x| \sigma^x_j \sigma^x_{j+1} + |J_y| \sigma^y_j \sigma^y_{j+1} \right) \ . \tag{2.11}$$

To understand the magnetic behaviour we can think about the spins in a classical sense. The first term wants to align spins along the x axis, however, the second one wants to do so along the y axis. So depending on the magnitude of the couplings, alignment along some direction in between should minimize the energy. Hence it makes sense that there is an ordered phase. Note that if we rotate all the spins by π around the z axis, we would get a configuration with the same energy. These two solutions correspond to Spontaneous Symmetry Breaking phases. By this we mean that the ground state breaks the $\mathbb{Z}_2$ symmetry of the Hamiltonian by choosing to be in one of these two states.

2.4 The Ising/Kitaev Chain

Another insightful example is the TFIM [21], by which we can, hopefully, explain many of the essential physics of the problem. In this case the Hamiltonian corresponds to $J_y = 0$ in Eq.2.1,

$$H_{TFIM} = -\sum_{j=1}^{L-1} J_x \sigma_j^x \sigma_{j+1}^x - h \sum_{j=1}^{L} \sigma_j^z \ . \tag{2.12}$$

We note that using an appropriate canonical transformation one can always set $J_x, h > 0$. For simplicity we also set $J_x = 1$ as a unit of our energy.

We start by looking at $h = 0$. This special point is quite simple to study and has many features which we are searching for like doubly degenerate ground state and MZMs. The Hamiltonian reads,

$$H_0 = -\sum_{j=1}^{L-1} \sigma_j^x \sigma_{j+1}^x \ . \tag{2.13}$$

This Hamiltonian is already diagonal and any product state in the x-basis is an eigenstate. The ground state is two-fold degenerate,

$$|G_R\rangle = |\rightarrow\rangle^{\otimes L}, \qquad |G_L\rangle = |\leftarrow\rangle^{\otimes L} \ . \tag{2.14}$$

The energy per bond is $\epsilon_b = -1$ and all the terms in the Hamiltonian are satisfied and have their lowest possible energy which gives total energy $E_0 = -(L-1)\epsilon_b = -(L-1)$.

One can see that $|G_R\rangle$ and $|G_L\rangle$ are not parity eigenstates, though it is possible to make common eigenstates of Hamiltonian and parity as follows,

$$\begin{aligned} |G, p = +1\rangle &= |\rightarrow\rangle^{\otimes L} + |\leftarrow\rangle^{\otimes L} \ , \\ |G, p = -1\rangle &= |\rightarrow\rangle^{\otimes L} - |\leftarrow\rangle^{\otimes L} \ . \end{aligned} \tag{2.15}$$

The model, Eq.2.13, is gapped. The easiest way to have an excitation is to create a domain wall,

$$|1dw_j\rangle = \rightarrow\rightarrow\rightarrow\cdots\rightarrow\rightarrow\wr\leftarrow\leftarrow\cdots\leftarrow\leftarrow\leftarrow \ , \tag{2.16}$$

in which the domain wall occurs between sites j and $j+1$. We have $L-1$ of these domain walls with the same energy, $\Delta E = 2$ with respect to ground state's energy. One can also consider its $\mathbb{Z}_2$ partner,

$$|1\tilde{dw}_j\rangle = \leftarrow\leftarrow\leftarrow\cdots\leftarrow\leftarrow\wr\rightarrow\rightarrow\cdots\rightarrow\rightarrow\rightarrow\ , \tag{2.17}$$

and construct a parity eigenstates from them,

$$\begin{aligned} |dw_j, p=+1\rangle &= |1dw_j\rangle + |1\tilde{dw}_j\rangle, \\ |dw_j, p=-1\rangle &= |1dw_j\rangle - |1\tilde{dw}_j\rangle\ . \end{aligned} \tag{2.18}$$

At this point, $h = 0$, one can see that the full spectrum is **exactly** doubly degenerate and each state has a partner with an opposite parity.

Now it is time to introduce the *Edge Operators*[§]. Consider the following operators,

$$\gamma_{A,1} = \sigma_1^x, \qquad \gamma_{B,N} = \left(\prod_{k=1}^{L-1}\sigma_k^z\right)\sigma_L^y\ . \tag{2.19}$$

It is straightforward to check that they satisfy following properties [22]:

1) They are conserved quantities, namely $[H, \gamma_{A,1}] = [H, \gamma_{B,L}] = 0$.

2) They are normalizable, i.e. $\gamma_{A,1}^2 = \gamma_{B,L}^2 = \mathbb{1}$.

3) They are real, i.e. $\gamma_{A,1} = \gamma_{A,1}^\dagger$ and $\gamma_{B,L} = \gamma_{B,L}^\dagger$.

4) They map states with opposite parity to each other, since they anticommute with the parity, $\{P, \gamma_{A,1}\} = \{P, \gamma_{B,L}\} = 0$ [¶].

Basically in the fermionic language these two MZMs can be combined and form a usual Dirac fermion, $f_0 = \frac{1}{2}(\gamma_{A,1} + i\gamma_{B,L})$. This fermionic state has zero energy, since $[H, f_0] = 0$. So all the states can be put in two classes in one of which the *zero energy* state is left to be empty and in the other set it is filled. Given a state in the former set, one can fill the zero energy state and find another state with the same energy in the latter set. This means that not only the ground state, but the full spectrum is doubly degenerate.

Now we look at the fermionic representation of H_0 and go through some details. The Hamiltonian reads,

$$H_0 = -\sum_{j=1}^{L-1}(c_j^\dagger - c_j)(c_{j+1}^\dagger + c_{j+1})\ . \tag{2.20}$$

[§]Actually edge operators up to a string which will disappear when we consider the model in the fermionic language. You can also find more about edge operators in the next chapter.

[¶]For example, $\gamma_{A,1}|GS, p=+1\rangle = |GS, p=-1\rangle$.

In general, the femionic representation of TFIM with OBC is called the *Kitaev Chain* [11](Eq.2.20 is a special case of it). Now we define Majorana fermions,

$$\gamma_{A,j} = c_j + c_j^\dagger,\ \gamma_{B,j} = \frac{c_j - c_j^\dagger}{i}\ , \tag{2.21}$$

$$\{\gamma_{r,i}, \gamma_{r',j}\} = 2\delta_{rr'}\delta_{ij}\ . \tag{2.22}$$

The Hamiltonian can be written in terms of Majoranas,

$$H_0 = \sum_{j=1}^{L-1} i\gamma_{B,j}\gamma_{A,j+1}\ . \tag{2.23}$$

First of all note that $\gamma_{A,1}$ and $\gamma_{B,L}$ do not appear in the Hamiltonian and they commute with it. We define new fermions,

$$\begin{aligned} f_1 &= \frac{1}{2}\left(\gamma_{A,1} + i\gamma_{B,L}\right)\ , \\ f_j &= \frac{1}{2}\left(\gamma_{A,j} + i\gamma_{B,j-1}\right),\ j \in \{2, 3, \ldots, L\}\ . \end{aligned} \tag{2.24}$$

With this definition we can rewrite the Hamiltonian as,

$$\begin{aligned} H_0 &= \sum_{n=2}^{L}(1 - 2f_n^\dagger f_n)\ , \\ &= (L-1) - 2\sum_{n=2}^{L} f_n^\dagger f_n\ , \end{aligned} \tag{2.25}$$

which does not depend on f_1. The ground state of H_0 is doubly degenerate. In one case one fills all the states correspond to new fermions, f_j-fermions in Eq.2.24. Filling the first state, $n = 1$, does not contribute to the energy, although for filling any other state we lower the energy by $\epsilon_n = -2$. Hence in total we have $E_0 = 0 + (L-1) - 2 \times (L-1) = -(L-1)$. The neat property is that we can also leave the $n = 1$ state to be empty and still get the same energy. So there are two ground states with energy $-(L-1)$ which differ in number of fermions, in other words they have different parity, $P_F = (-1)^{N_f}$. We were successful in deriving the same result as in the spin language.

The fascinating feature is that the f_1 state includes Majoranas from both edges, *half* of it lives on the left edge and the other half on the right one. As we will see in next sections, such a *non-local* state is always present in the topological phase and can be viewed as a topological qubit. The difference between the two states of the qubit lies in whether the $n = 1$ state is filled or not. Furthermore such a qubit is immune to perturbations in the bulk, however, one can change it by operations on the edges.

Now we move on and study the other limiting case. For $h \gg J_x$ in Eq. 2.12 we can drop the first term and study the second term,

$$H_\infty = -h \sum_{j=1}^{L} \sigma_j^z \ . \tag{2.26}$$

The ground state of this model is unique and it depends on the direction of magnetic field. For $h > 0$, the ground state is $|\uparrow\rangle^{\otimes L}$. In this case the parity of the ground state is, $p = (+1)^L = +1$. For $h < 0$ the ground state is $|\downarrow\rangle^{\otimes L}$. In this case, contrary to the previous case, the parity **does depend** on the number of sites, $p = (-1)^L$, which is $+1$ for an *even* number of sites and -1 for an *odd* number of them. Apart from these details, the important feature is the uniqueness of the ground state. No matter whether one has even or odd number of sites, no matter h is positive or negative, **the ground state is unique**. This is the paramagnetic or disordered phase[§]. This phase is also gapped, as one can see for $h > 0$ the easiest excitation is flipping one spin which gives rise to $+2h$ energy with respect to the ground state energy and this shows that the paramagnetic phase is also gapped.

The full Hamiltonian of the TFIM with OBC, 2.12, is also solvable by means of the JW transformation which maps the magnetic field term to a chemical potential term in the fermionic language. This is not an easy task due to lack of a good quantum number like momentum for a closed chain. Nevertheless, Lieb et al [20] came up with a method which is essentially a Bogoliubov transformation in real space. This transformation introduces a *label* for each state which plays the role of momentum for an open chain. One can write all the wavefunctions in terms of this label. The allowed values of this label should be found by boundary conditions which naturally appear in the equations. Pfeuty used this method and solved the TFIM [21][¶] .

The TFIM has two phases and we have studied a simple representative Hamiltonian in each phase. The behaviour which has been explained for $h = 0$, is true for all values of magnetic field satisfying $|h| < |J_x|$. In this regime of parameters the system has two degenerate ground states in the thermodynamic limit, however, for any finite system size there are two *almost* degenerate ground states, the energy splitting of which, ε, is exponentially small in the system size, $\varepsilon \sim e^{-L/\xi}$ with $\xi > 0$. These two ground states are separated by finite energy gap, Δ, from the rest of the spectrum, $\varepsilon \ll \Delta$. Moreover, the spectrum can be divided to two sectors with different parities and each state has a partner with opposite parity in an $|\varepsilon|$ window around it.

The model with OBC has two MZMs localized on the edges with a tail in the bulk. For $h = 0$ we just had $\gamma_{A,1}$ on the left edge. Turning on h will result

[§]Note that the order parameter is $\langle \sigma_j^x \rangle$ which is zero.

[¶]We solved the full model 2.1 using the same method as well.

in having new terms in the bulk,

$$\gamma_L = \frac{1}{\mathcal{N}}\left[\gamma_{A,1} + \frac{h}{J_x}\gamma_{A,2} + \left(\frac{h}{J_x}\right)^2 \gamma_{A,3} + \dots\right] , \tag{2.27}$$

in which $\mathcal{N}$ is for normalization, $\gamma_L^2 = \mathbf{1}$. One can see that this operator is normalizable for $|\frac{h}{J_x}| < 1$, which is the topological phase. At the critical point, $|h| = |J_x|$ the model becomes gaplees . For $|h| > |J_x|$ we are in the disordered phase of the model and expect no MZM at all. The fact that the operator, γ_L, is not normalizable in this regime confirms our prediction.

Due to the difficulties of solving the probelm with OBC it is natural to ask how one can determine the presence of the zero mode in an open chain by looking at the closed one which is easy to solve. Note that solving the problem on a ring will give us a clue about the presence or absence of the MZM if one opens the chain, but it **does not** give us neither wavefunctions nor the localization length of MZM [11]. Should you need details of MZMs, there is no other option rather than solving the problem with OBC.

Therefore we close this section by presenting an easy and useful method to determine whether the system is in the topological or trivial phase Using a Fourier transformation, $c_k = \frac{1}{L}\sum_k e^{ikj} c_j$, we can write the Hamiltonian of the Kitaev chain on a ring,

$$\begin{aligned} H_C &= \frac{1}{2}\sum_k (c_k^\dagger,\ c_{-k}) \begin{pmatrix} 2h - 2J_x\cos k & -2iJ_x \sin k \\ 2iJ_x \sin k & 2J_x\cos k - 2h \end{pmatrix} \begin{pmatrix} c_k \\ c_{-k}^\dagger \end{pmatrix} \\ &= \frac{1}{2}\sum_k \Psi_k^\dagger \mathcal{H}_k \Psi_k \ , \end{aligned} \tag{2.28}$$

in which $\Psi_k = (c_k,\ c_{-k}^\dagger)^T$ and values of k depends on the periodic or anti-periodic boundary condition. We can rewrite $\mathcal{H}_k$ in terms of Pauli matrices, $\boldsymbol{\tau}$ which act on the Ψ_k space,

$$\begin{aligned} &\mathcal{H}_k = \mathbf{h}(k)\cdot\boldsymbol{\tau}, \\ &\mathbf{h}(k) = (0, 2J_x\sin k, 2h - 2J_x\cos k) \ . \end{aligned} \tag{2.29}$$

If one considers the thermodynamic limit the wavevector k spans the full $[0, 2\pi]$ interval as opposed to a finite set of points. Therefore one can ask how many times does $\mathbf{h}(k)$ wind around the origin in the $z-y$ plane if one changes k from 0 to 2π? Let us first look at limiting cases. For $h = 0$ the vector winds once around the origin[§], however, for $|h| \gg |J_x|$ the vector is far from the origin and does not wind at all. Thus in the topological phase the winding number is ± 1 and it is 0 in the trivial phase. The winding number is an integer

[§]Whether it is clockwise or anticlockwise depends on the sign of J_x and how one defines the axes.

and it can only change when the gap closes, namely $|h| = |J_x|$. Although the winding number is defined for the closed chain, it has also a meaning for the open chain. In the topological phase, the non-zero winding number tells how many MZMs one gets on the edges of an open chain. In our example, the winding number is 1 in the topological phase and as we have seen there is one MZM on each edge[§]. In the trivial phase the winding number is 0 and there is no MZM at all!

2.5 The paper in almost plain English

In this section we give a short summary of our results, details of which can be found in the paper.

The XY model and TFIM both were solved for an open chain [20, 21] based on which one can deduce the wavefunctions of the MZMs. Using the same method as previous studies, we solved the full model for an open chain analytically. We present all the eigenvalues and wavefunctions, specially for the MZMs in the topological region. Here is the brief version of it.

We want to solve the full Hamiltonian in Eq.2.6,

$$H = \frac{1}{2}\sum_{j=1}^{L-1}(c_j^\dagger c_{j+1} + \Delta c_j^\dagger c_{j+1}^\dagger + h.c.) - \mu\sum_{j=1}^{L}(c_j^\dagger c_j - \frac{1}{2}) \ .$$

Solving the model on a ring is straight forward since it can be mapped to a quadratic Hamiltonian, H_C, in Eq.2.28 but finding the excitations with OBC is not an easy task as it was for the case $J_y = h = 0$, since the momentum is not a good quantum number for an open chain. As we mentioned earlier, another method has been used by Lieb et al [20] (LSM method) to solve the XY model and can be used here as well. Though applying it for the current problem is not straightforward, understanding the general idea is rather simple.

In the periodic case one uses a Bogoliubov transformation to diagonalize the Hamiltonian, Eq.2.28, and allowed values of momentum can be fixed by the boundary condition, either periodic or anti-periodic. The same strategy, though with a little bit more calculation, works for an open chain as well.

The dispersion relation for the full model on a ring is,

$$\omega_k^2 = (\mu - \cos k)^2 + \Delta^2 \sin^2 k \ . \tag{2.30}$$

To solve the problem with OBC, one considers a *Bogoliubov-like* transformation in real space which diagonalizes the Hamiltonian. Crucially, one assumes that *the functional form of the dispersion relation is still the same,*

[§]In principle one could have as many Majorana as desired. We will look at one such example in next section details of which is presented in the paper.

though one needs to use a new label, say α, which takes the roll of momentum,

$$\eta_\alpha = \sum_{i=1}^{L} (g_{\alpha,i} c_i + h_{\alpha,i} c_i^\dagger), \tag{2.31}$$

$$H = \sum_{\alpha=1}^{L} \Lambda_\alpha \eta_\alpha^\dagger \eta_\alpha, \;\; \Lambda_\alpha > 0 \;, \tag{2.32}$$

$$\Lambda_\alpha^2 = (\mu - \cos\alpha)^2 + \Delta^2 \sin^2\alpha \;, \tag{2.33}$$

in which $g_{\alpha,i}$ and $h_{\alpha,i}$ are two functions which should be determined. Note that there could be some constant energy term in the Hamiltonian which can be neglected and the transformation is canonical, so η_α operators satisfy the usual spinless fermionic algebra. We used the LSM method and derived the wavefunctions, $g_{\alpha,i}$ and $h_{\alpha,i}$, and an equation that fixes the possible values of α. Therefore we have determined all the states ananlytically, namely all wavefunctions and their corresponding energy, for arbitrary Δ and μ. In what follows we focus on the ground state and MZMs.

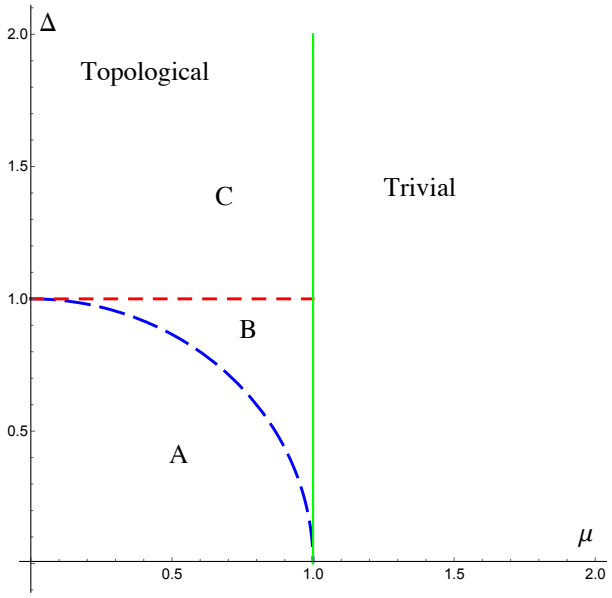

Figure 2.1: Phase diagram for Kitaev chain. For $|\mu| < 1$ system is in the topological phase which itself divided to three regions, A, B and C, due to differences in Majorana zero mode's wavefunction.

We summerize the phase diagram and MZM's wavefunctions in Fig. 2.1 [§]. At the origin $\Delta = \mu = 0$ and the μ-axis we have a simple cosine band

[§]Based on either a gauge transformation or mapping solutions to each other, as is explained in the paper, one can show that studying $\Delta, \mu > 0$ is sufficient.

and the Δ-axis is the XY model. The TFIM has $\Delta = 1$ and is depicted by the red dashed line. The line $\mu = 1$ is a gapless line which is described by theIsing CFT [24]. For $\mu > 1$ the system is in the trivial phase, hence there is no MZM at all. We divide the $\mu < 1$ region, the topological phase, to three parts, A, B and C, each of which has its own MZM's wavafunction. In the paper we explain details of the calculation and present all the wavefunctions. Here as an example, one can find the left MZM's wavefunction in region B where $\Delta < 1$ and $\sqrt{1-\Delta^2} < \mu < 1$,

$$\gamma_{L,\alpha^*} = \frac{1}{\mathcal{N}} \sum_{n=1}^{L} e^{-\frac{n}{\xi_1}} \sinh(\frac{n}{\xi_2}) \gamma_{A,n} \ , \tag{2.34}$$

$$\cosh \frac{1}{\xi_1} = \frac{1}{\sqrt{1-\Delta^2}}, \ \cosh \frac{1}{\xi_2} = \frac{\mu}{\sqrt{1-\Delta^2}} \ , \tag{2.35}$$

$$\alpha^* = i(\frac{1}{\xi_1} + \frac{1}{\xi_2}) \ , \tag{2.36}$$

in which $\mathcal{N}$ is a normalization constant. It is clear that this MZM is localized on the left edge and it is a zero mode indeed, i.e. $\Lambda_{\alpha^*} = 0$.

We have also studied the model with longer range couplings [25, 26]. This gives us the possibility of having more MZMs on each edge since topological phases of superconductors with time-reversal and particl-hole symmetry, i.e. class **BDI**, in one dimension are classified by $\mathbb{Z}$ [27]. Following Niu et al [25] we consider a Hamiltonian with equal hopping and pairing couplings,

$$\begin{aligned} H = & \frac{t}{2} \sum_{j=1}^{L-1} (c_j^\dagger c_{j+1} + c_j^\dagger c_{j+1}^\dagger + h.c.) \\ & + \frac{\lambda}{2} \sum_{j=1}^{L-2} (c_j^\dagger c_{j+2} + c_j^\dagger c_{j+2}^\dagger + h.c.) \\ & - \mu \sum_{j=1}^{L} (c_j^\dagger c_j - \frac{1}{2}) \ . \end{aligned} \tag{2.37}$$

where λ is the next nearest neighbor(NNN) hopping and pairing amplitude. We perform the Fourier transformation which allows us to compute the phase diagram using winding number method,

$$\begin{aligned} H_C &= \frac{1}{2} \sum \Psi_k^\dagger \mathcal{H}_k \Psi_k, \\ \mathcal{H}_k &= [-t \sin(k) - \lambda \sin(2k)] \tau^y \\ &\quad + [t \cos(k) + \lambda \cos(2k) - \mu] \tau^z \ . \end{aligned} \tag{2.38}$$

The phase diagram is given in Fig.2.2. The gap closes when $\lambda = \mu \pm t$ and $\lambda = \mu$ for $|t| < 2|\mu|$. At the origin we only have chemical potential so it is

natural to be in the trivial phase where there is no MZM. For large NN terms, $|t| \gg |\lambda|, |\mu|$, we retrieve the special point of the Kitaev chain as discussed in the previous section for which the model hosts one MZM on each end. In the other limit, $|\lambda| \gg |t|, |\mu|$, we would get two decoupled Kitaev chains, one for odd sites and one for even sites. Therefore in this limit two MZMs live on each edge. The Interested reader can find the MZM wavefunctions in both topological phases in the paper.

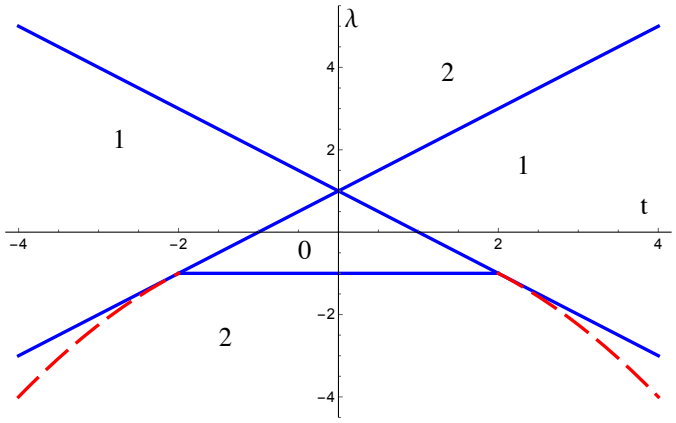

Figure 2.2: Phase diagram for Kitaev chain with NNN terms for $\mu = 1$. The numbers in the plot show the number of Majorana zero modes at each end of the chain. The red lines separate regions in which the wavefunctions of the MZMs behave differently as explained in the paper.

Now one could ask what would happen if we break the time-reversal symmetry? Well, form the classification scheme [27] we know that in this case the phases are classified by $\mathbb{Z}_2$ which means that at most one could get one MZM on each edge. Sticlet et al [26] considered a special example, a chain with constant phase gradient in the pairing term,

$$\begin{aligned} H = & \frac{t}{2}\sum_{j=1}^{L-1}(c_j^\dagger c_{j+1} + e^{ij\nabla\theta}c_j^\dagger c_{j+1}^\dagger + h.c.) \\ & + \frac{\lambda}{2}\sum_{j=1}^{L-2}(c_j^\dagger c_{j+2} + e^{ij\nabla\theta}c_j^\dagger c_{j+2}^\dagger + h.c.) \\ & - \mu\sum_{j=1}^{L}(c_j^\dagger c_j - \frac{1}{2}) \ , \end{aligned} \tag{2.39}$$

in which $\nabla\theta$ is phase gradient. To proceed it is convenient to use our freedom

and transform operators as $c_j \to e^{ij\frac{\nabla\theta}{2}} c_j$ which results in,

$$\begin{aligned} H = & \frac{t}{2}\sum_{j=1}^{L-1}(e^{i\frac{\nabla\theta}{2}} c_j^\dagger c_{j+1} + e^{-i\frac{\nabla\theta}{2}} c_j^\dagger c_{j+1}^\dagger + h.c.) \\ & + \frac{\lambda}{2}\sum_{j=1}^{L-2}(e^{i\nabla\theta} c_j^\dagger c_{j+2} + e^{-i\nabla\theta} c_j^\dagger c_{j+2}^\dagger + h.c.) \\ & - \mu\sum_{j=1}^{L}(c_j^\dagger c_j - \frac{1}{2}) \ . \end{aligned} \tag{2.40}$$

In this Hamiltonian, although the hopping is also complex, all couplings are constant.

An interesting observation by Sticlet and colleagues was that in a finite region of the couplings one gets two MZM on one edge, say one localized Dirac fermion with zero energy on the left edge whereas there is no MZM on the right side. There is an easy way to see this for a special case, $\nabla\theta = \pi$ and $\mu = 0$[§],

$$H = \frac{t}{2}\sum_{j=1}^{N-1} i\gamma_{B,j}\gamma_{B,j+1} + \frac{\lambda}{2}\sum_{j=1}^{N-2} i\gamma_{B,j}\gamma_{A,j+2} \ , \tag{2.41}$$

in which $\gamma_{A,1}$ and $\gamma_{A,2}$ do not enter the Hamiltonian, however, $\gamma_{B,L-1}$ and $\gamma_{B,L}$ do appear.

This can not be related to topology. The system is in the trivial phase, because if it was in the topological phase, it would host a MZM on both edges not only on one of them. In other words, if the system was in the topological phase, the *topological number*, say the winding number, would change when one enters the vacuum from each end of the chain, hence something should happen on both ends in topological phase not only one of them!

As we show in the paper, for the Hamiltonian in Eq.2.40, one gets the same phase diagram as Fig.2.2, if one replaces $t \to t\cos\left(\frac{\nabla\theta}{2}\right)$ and $\lambda \to \lambda\cos\nabla\theta$. This shows that if one calculates the winding number, the resulting numbers would be the same. We should, however, read everything modulo 2 since in this case by breaking time-reversal symmetry we are in class **D** for which phases are classified by $\mathbb{Z}_2$ [27]. This means that any 2 in Fig.2.2, now with effective couplings, should be translated to 0 which is the trivial phase, though 1 still indicates the topological phase.

The root of one-sided zero energy fermionic mode is the fine-tuning of the couplings. To understand this phenomena we start by looking at the case with $\lambda = 0$. In this case one can calculate the wavefunction of MZMs (setting

[§]By looking at Eq.2.39 one can see that for this point the Hamiltonian has time-reversal symmetry though couplings are staggered.

$t = 1$),

$$\gamma_L = L \sum_{n=1}^{n=N} \Big[\frac{\mu}{\cos(\frac{\nabla\theta}{2})}\Big]^n \gamma_{A,n} \ , \tag{2.42}$$

$$\gamma_R = R \sum_{n=1}^{n=N} \Big[\frac{\mu}{\cos(\frac{\nabla\theta}{2})}\Big]^{N-n+1} [\sin(\frac{\nabla\theta}{2})\gamma_{A,n} + \cos(\frac{\nabla\theta}{2})\gamma_{B,n}], \tag{2.43}$$

in which L and R are normalization constant necessary to satisfy $\gamma_L^2 = \gamma_R^2 = \mathbf{1}$. We should mention that γ_L lives on the left edge, γ_R lives on the right edge and the topological phase is shrunk to the region $|\mu| < |\cos(\frac{\nabla\theta}{2})|$ in comparison to $|\mu| < 1$ which is the case for $\nabla\theta = 0$. The crucial difference here is that γ_L does only depend on $\gamma_{A,n}$, but γ_R has contributions from both $\gamma_{A,n}$ and $\gamma_{B,n}$.

Now we write the full Hamiltonian, Eq.2.40, in terms of Majorana fermions:

$$\begin{aligned} H = &-\frac{t}{2}\cos(\frac{\nabla\theta}{2}) \sum_{j=1}^{N-1} i\gamma_{B,j}\gamma_{A,j+1} \\ &+ \frac{t}{2}\sin(\frac{\nabla\theta}{2}) \sum_{j=1}^{N-1} i\gamma_{B,j}\gamma_{B,j+1} \\ &- \frac{\lambda}{2}\cos(\nabla\theta) \sum_{j=1}^{N-2} i\gamma_{B,j}\gamma_{A,j+1} \\ &+ \frac{\lambda}{2}\sin(\nabla\theta) \sum_{j=1}^{N-2} i\gamma_{B,j}\gamma_{B,j+1} \\ &- \frac{\mu}{2} \sum_{j=1}^{N} i\gamma_{A,j}\gamma_{B,j} \ . \end{aligned} \tag{2.44}$$

We can understand the phenomena with the following picture. If we start from $t = 0$, we would have two decoupled chains with a phase gradient. By looking at Eq.2.44 we see that by turning on t which couples two chains, γ_B at different sites starts to talk with each other. Since γ_R from these two chains have γ_B contributions, they start to talk as well and hence they will be gapped out. The γ_A operators, however, are not coupled. Therefore two γ_L operators can survive, though with a modified wavefunction. The fine-tuning of parameters ensures that the Hamiltonian is free of terms like $\gamma_{A,n}\gamma_{A,n+1}$ and this assures that two MZMs survive on the left side. In the paper by solving equations which govern MZMs, resulting in analytical wavefunctions, we show how one can derive the *effective* phase diagram as well as MZMs' wavefunctions.

3

Zero Modes Of Interacting Models

3.1 Introduction

In the previous chapter we were studying a free model. The natural question is what does happen if one adds interactions to the model? Will there be any topological phase? Will MZMs survive?

Here we will look at one example[§], for which one can find the ground states exactly. The model is gapped and it has a doubly degenerate ground state with different parities [30–32], for which people generally call them topological.

Obtaining MZM wavefunctions is not as easy as in the non-interacting case. One way to construct MZMs is by using perturbation theory, as Fendley did previously for the TFIM, clock models [22] and the XYZ spin chain [33]. To construct MZM with perturbation for the TFIM, Fendley started from the $h = 0$ case for which we know the MZM, namely $\gamma_{A,1}$. Most importantly we have $[\gamma_{A,1}, H_{TFIM}|_{h=0}] = 0$. Now we can turn on the magnetic field and calculate $[\gamma_{A,1}, H_{TFIM}] = 2ih\gamma_{B,1}$, which is first order in h. In the next step one can consider $\Gamma = \gamma_{A,1} + h\gamma_{A,2}$, for which we have $[\Gamma, H_{TFIM}] = \mathcal{O}(h^2)$. It is possible to continue this procedure step by step and at the $n-th$ step find an operator such that its commutator with the Hamiltonian is $\mathcal{O}(h^n)$. Moreover one can see that this operator is normalizable. Fendley constructed the edge zero modes of XYZ model, which is an interacting model though integrable, using this perturbative method. The neat feature is that the edge operator is only normalizable within the ordered/topological phase. The direct implication of the presence of such an operator is the two-fold degeneracy of the full spectrum of the model with open boundary condition.

Fendley did the same type of perturbative calculation for the clock models as well [22] based on which he proposed that these models also have edge zero modes, though in this case they are *Parafermions* due to which one gets a three-fold degeneracy in the full many-body spectrum [19, 22]. For instance,

[§]In one dimension we know that for **BDI** class the $\mathbb{Z}$ classification reduces to $\mathbb{Z}_8$ [28, 29].

in the 3-state **chiral** Potts model, one would get a triple degeneracy in the full spectrum, all the way to highest excited state. If such an operator exists, like what we mentioned for the TFIM and XYZ models, we say that the model has a **Strong** Zero Mode. On the other hand a new study claims that due to appearance of resonances the strong zero mode can only exist in very specific points of chiral model [34].

Another way to approach the problem is by focusing on the ground state subspace and find an operator such that it changes the parity and maps different ground states to each other. Katsura et al [31] took this way and adiabatically connected an interacting model to a free one such that the ground state remained the same. In the free model one can calculate the MZM easily. Therefore one has MZMs such that only connect the ground states of the interacting model, which is called **Weak** zero mode.

In this chapter we will first look at an example of an interacting $\mathbb{Z}_2$ symmetric model and present the ground states as well as the weak zero modes. After that we will propose a $\mathbb{Z}_3$ symmetric model for which the ground state is three fold degenerate and known exactly. This work is in the progress and we are exploring different aspects of it.

3.2 "Have you looked a two-site problem?"

As a $\mathbb{Z}_2$ symmetric model we study the TFIM and add a nearest neighbour interaction as follows,

$$\begin{aligned} H &= \sum_{j=1}^{\tilde{L}} h_{j,j+1} \ , \\ h_{j,j+1} &= -\sigma_j^x \sigma_{j+1}^x + \frac{h}{2}(\sigma_j^z + \sigma_{j+1}^z) + U\sigma_j^z \sigma_{j+1}^z \ , \end{aligned} \tag{3.1}$$

in which U is a new coupling constant and L is the number of sites. For an open chain $\tilde{L} = L - 1$, however, for a closed chain $\tilde{L} = L$. From the JW transformation one finds that this Hamiltonian describes fermions with $n_j n_{j+1}$ interaction. Note that for a closed chain all the spins have the same magnetic field, h, but in the open chain, the first and the last spin have a magnetic field half the value of the magnetic field for the bulk spins. We do not expect that this modification on the edges changes the phase diagram of the model, however, it *does* change details of ground states and edge modes.

For $h = U = 0$ we know that $|\rightarrow\rangle^{\otimes L}$ and $|\leftarrow\rangle^{\otimes L}$ are eigenstates. One can ask that if it is possible to tune couplings to have product states as the ground states? To show that the answer is positive we follow Katsura et al [31] [§].

[§] In the original paper by Peschel and Emery, an other method was used.

We consider the two-body Hamiltonian and we note that parity is a good quantum number. In the even sector we have,

$$h^e_{j,j+1} = \begin{array}{c} \begin{array}{cc} |\uparrow\uparrow\rangle & |\downarrow\downarrow\rangle \end{array} \\ \begin{pmatrix} U+h & -1 \\ -1 & U-h \end{pmatrix} \end{array} . \tag{3.2}$$

The lowest eigenestate of this Hamiltonian is,

$$\epsilon_e = U - \sqrt{1+h^2}, \qquad |\psi_e\rangle \sim |\uparrow\uparrow\rangle + \left(h + \sqrt{1+h^2}\right)|\downarrow\downarrow\rangle \ . \tag{3.3}$$

In the odd sector we have,

$$h^o_{j,j+1} = \begin{array}{c} \begin{array}{cc} |\uparrow\downarrow\rangle & |\downarrow\uparrow\rangle \end{array} \\ \begin{pmatrix} -U & -1 \\ -1 & -U \end{pmatrix} \end{array} . \tag{3.4}$$

The lowest eigenestate in this case is,

$$\epsilon_o = -U - 1 \qquad |\psi_o\rangle \sim |\uparrow\downarrow\rangle + |\downarrow\uparrow\rangle \ . \tag{3.5}$$

Now we demand two things. First of all the two eigenvalues should be equal, and second we should be able to write down some combination of eigenvectors such that it becomes a product state. The first constraint is,

$$\begin{aligned} \epsilon_e &= \epsilon_o \ , \\ \Rightarrow \ 2U + 1 &= \sqrt{1+h^2} \ . \end{aligned} \tag{3.6}$$

This equation shows that the sign of h is not important, but U should be positive. This can be easily understood by considering the following transformation,

$$\begin{aligned} \sigma^x_j &\to \sigma^x_j, \\ \sigma^y_j &\to -\sigma^y_j, \\ \sigma^z_j &\to -\sigma^z_j \ . \end{aligned} \tag{3.7}$$

This transformation only changes the sign of magnetic field in the model.

We need to check the second condition as well,

$$|\psi_e\rangle + x|\psi_o\rangle = (|\uparrow\rangle + \alpha|\downarrow\rangle) \otimes (|\uparrow\rangle + \alpha|\downarrow\rangle) \ , \tag{3.8}$$

in which x and α are unknown.

One can check that both requirements, Eqs.3.6 and 3.8, can be satisfied by the following choice,

$$U = \frac{1}{2}\left[\cosh(l) - 1\right], \qquad h = \sinh(l) \ , \tag{3.9}$$

$$x = \alpha^2 = e^l, \quad l \geq 0 \ . \tag{3.10}$$

This means that there is a one parameter line in the $h-U$ plane for which the ground state is doubly degenerate,

$$|\psi^{+}(l)\rangle = (|\uparrow\rangle + \alpha|\downarrow\rangle)^{\otimes L}, \quad |\psi^{-}(l)\rangle = (|\uparrow\rangle - \alpha|\downarrow\rangle)^{\otimes L} \ , \tag{3.11}$$

in which and from now on $\alpha = e^{l/2}$. This line is known as the **Peschel-Emery**(PE) line [30]. Note that these are the ground states for an open as well as a closed chain, by construction.

One can construct parity eigenstates as well,

$$|P = \pm 1(l)\rangle = |\psi^{+}(l)\rangle \pm |\psi^{-}(l)\rangle \ . \tag{3.12}$$

Using the JW transformation one can write these wavefunctions in the fermionic language for an open chain [31],

$$\begin{aligned}
|\psi^{\pm}\rangle &= (|\uparrow\rangle \pm \alpha|\downarrow\rangle)^{\otimes L} \\
&= \left[\mathbf{1} \pm \alpha\sigma_1^-\right]\left[\mathbf{1} \pm \alpha\sigma_1^z\sigma_2^-\right]\ldots \\
&\left[\mathbf{1} \pm \alpha\left(\prod_{i_{L-1}=1}^{L-2}\sigma_{i_{L-1}}^z\right)\sigma_{L-1}^-\right]\left[\mathbf{1} \pm \alpha\left(\prod_{i_L=1}^{L-1}\sigma_{i_L}^z\right)\sigma_L^-\right]|\uparrow\rangle^{\otimes L} \\
&= (1 \pm \alpha c_1^\dagger)(1 \pm \alpha c_2^\dagger)\ldots(1 \pm \alpha c_{L-1}^\dagger)(1 \pm \alpha c_L^\dagger)|0\rangle^{\otimes L} \\
&= e^{\pm\alpha c_1^\dagger}e^{\pm\alpha c_2^\dagger}\ldots e^{\pm\alpha c_{L-1}^\dagger}e^{\pm\alpha c_L^\dagger}|0\rangle^{\otimes L} \ ,
\end{aligned} \tag{3.13}$$

in which $\sigma^- = (\sigma^x - i\sigma^y)/2$. Now it is evident that $|P=+1\rangle$ has even number of fermions and $|P=-1\rangle$ has odd number of them, just like what we had in the TFIM.

It can be shown that the weak zero mode for an open chain which lives on the left side is the following operator,

$$W_L = \frac{1}{\sqrt{1+q^2+\cdots+q^{2(L-1)}}}\sum_{n=1}^{L} q^{n-1}\left(\prod_{j=1}^{n-1}\sigma_j^z\right)\sigma_n^x \ , \tag{3.14}$$

$$q = \frac{1-\alpha^2}{1+\alpha^2} \ . \tag{3.15}$$

One can see that $|q|<1$ which ensures that the operator is localized on the left edge. This operator is a Majorana operator, $W_L^\dagger = W_L$ and $W_L^2 = \mathbf{1}$, and maps ground states with different parities to each other **exactly**.

3.3 The Paper in Plain English

We have asked how one can generalize the PE line to other models? Is it possible to have it for spin-S chains? Is it possible to have it for clock models which have not been solved yet, except for the integrable cases?

Previously the spin-S generalization of PE line has been discussed [35–37]. We found the exact and compact form of ground states and edge modes. The Hamiltonian for each link for spin-S model is,

$$h^{S-PE}_{j,j+1} = -S^x_j S^x_{j+1} + \frac{h(l)}{2} S\left(S^z_j + S^z_{j+1}\right) + U(l) S^z_j S^z_{j+1} \ , \tag{3.16}$$

where S^α form the spin-S representation of $SU(2)$ algebra and one uses the same $h(l)$ and $U(l)$ as in Eq.3.9. In this case the $\mathbb{Z}_2$ symmetry is the parity of the magnetization, $P_M = \prod_{j=1}^{L} e^{i\pi(S-S^z_j)}$. One can see that the first term either does not change the magnetization or change it by two, hence the parity of magnetization is a conserved quantity. The ground states are,

$$|\psi^{\pm}_S(l)\rangle = \left(e^{\pm\alpha S^-}|S\rangle_z\right)^{\otimes L} \ , \tag{3.17}$$

where as before $\alpha = \exp(l/2)$, $|S\rangle_z$ is the $S_z = S$ eigenstate and the energy per bond is, $\epsilon_S(l) = -S^2(U(l)+1)$ [§].

We mention that we found some exact excited states for this model for all values of S. These states have energy $\Delta E = 2S$. In the case of $S = \frac{1}{2}$ we obtained some additional states. One can find all of these states in the paper.

We have also considered the generalization to the 3-state clock model. For clock-like models it would be fruitful to have a model for which at least the ground state is known exactly as is the case for the AKLT model [38, 39].

We need to define the basic operators for the 3-state clock model. We can think of σ^z as an operator which has square roots of 1 as its diagonal elements, so we define Z to have *cube* roots of 1,

$$Z = \begin{pmatrix} 1 & 0 & 0 \\ 0 & \omega & 0 \\ 0 & 0 & \bar{\omega} \end{pmatrix} \ , \tag{3.18}$$

in which $\omega = \exp(\frac{2\pi i}{3})$. To generalize σ^x the best way is considering it as *spin flip* which changes to a *shift* operator,

$$X = \begin{pmatrix} 0 & 1 & 0 \\ 0 & 0 & 1 \\ 1 & 0 & 0 \end{pmatrix} \ . \tag{3.19}$$

It is staright forward to check that $Z^3 = X^3 = \mathbf{1}$ and $XZ = \omega ZX$.

Now we can define the corresponding *transverse field* model, known as Potts or Clock model,

$$H = -\sum_{j=1}^{L-1}(X^\dagger_j X_{j+1} + h.c.) - f\sum_{j=1}^{L}(Z^\dagger_j + h.c.) \ . \tag{3.20}$$

[§]For spin-$\frac{1}{2}$ this Hamiltonian is $\frac{1}{4}$ of the the Hamiltonian in Eq.3.1.

It is known that for $|f| < 1$ this model has 3 degenerate ground states and for $|f| > 1$ it has a paramagnetic phase. An easy way to see this is using duality transformation.

Fendley suggested [22] that the chiral Potts model in which $X^\dagger X \rightarrow e^{i\theta} X^\dagger X$ for real θ hosts *parafermionic* edge zero modes with localization length of the order of $f/\sin(3\theta)$, which makes the whole many-body spectrum triply degenerate; just like MZMs! However, as we mentioned earlier, a recent study [34] shows that the only candidate point to be able to have such three fold degenerate spectrum is $\theta = \pi/6$ for which Fendely's calculation also shows the best localization on the edges.

Our goal is to modify the Potts model and come up with an analogue of the PE line. The Potts model, even the chiral one, has $\mathbb{Z}_3$ symmetry, namely the parity $P = \prod_{j=1}^{L} Z$ which commutes with the Hamiltonian. Since $P^3 = \mathbf{1}$, we can assign a parity to each state, $P = \omega^Q$ where Q could be 0, 1 and 2. We want to keep this symmetry, add some terms and find a manifold-which turns out to be a line- such that the ground state is three fold degenerate and has a product state form. We borrow our knowledge from the PE line and add ZZ and $ZZ^\dagger$ terms - in analogy with $\sigma^z\sigma^z$ term- which respect the $\mathbb{Z}_3$ symmetry as follows,

$$\begin{aligned} H =& \sum_j h_{j,j+1} \ , \\ h^{Z_3}_{j,j+1}(r) =& - X_j^\dagger X_{j+1} - f(r)(Z_j + Z_{j+1}) \\ & - g_1(r) Z_j Z_{j+1} - g_2(r) Z_j Z_{j+1}^\dagger + h.c. \ . \end{aligned} \tag{3.21}$$

Demanding for a product state gave us a line parametrized with $r > 0$,

$$f(r) = (1+2r)(1-r^3)/(9r^2) \ , \tag{3.22}$$

$$g_1(r) = -2(1-r)^2(1+r+r^2)/(9r^2) \ , \tag{3.23}$$

$$g_2(r) = (1-r)^2(1-2r-2r^2)/(9r^2) \ . \tag{3.24}$$

Along this line the model has three degenerate ground states,

$$|G_0(r)\rangle = (|0\rangle + r|1\rangle + r|2\rangle)^{\otimes L} \ , \tag{3.25}$$

$$|G_1(r)\rangle = (|0\rangle + r\omega|1\rangle + r\bar{\omega}|2\rangle)^{\otimes L} \ , \tag{3.26}$$

$$|G_2(r)\rangle = (|0\rangle + r\bar{\omega}|1\rangle + r\omega|2\rangle)^{\otimes L} \ , \tag{3.27}$$

with the energy per bond $\epsilon_b(r) = -2(1+r+r^2)^2/(9r^2)$. As was the case for the PE line we can also combine these states to have eigenstates with definite parity,

$$|Q=0\rangle = |G_0(r)\rangle + |G_1(r)\rangle + |G_2(r)\rangle \tag{3.28}$$

$$|Q=1\rangle = |G_0(r)\rangle + \bar{\omega}|G_1(r)\rangle + \omega|G_2(r)\rangle \tag{3.29}$$

$$|Q=2\rangle = |G_0(r)\rangle + \omega|G_1(r)\rangle + \bar{\omega}|G_2(r)\rangle \ . \tag{3.30}$$

Finally we note that for this model we have also found edge operators which are normalizable though they are not parafermions, as well three exact excited states with energy $\epsilon(r) + 2 + r$. For details we refer to the paper.

4

Conclusion and Outlook

We have looked at free and interacting models of fermions with $\mathbb{Z}_2$ symmetry. We have found the MZM's wavefunction for the Kitaev chain as well as the *weak* zero mode of an interacting $\mathbb{Z}_2$ symmetric chain. However, it is still interesting to know if there is a *strong* zero mode for these interacting models. Fendley found an example of it for the XYZ chain [33], which is an integrable model. We have been working on a non-integrabel model, namely the TFIM with an interaction, which could make the problem different. Nevertheless, we have seen some features of strong zero mode along the PE line in numerics. For instance, we have seen that the spectrum is almost doubly degenerate up to the highest excited states as well as long-time correlation of edge magnetization [40]. On the other hand we have an argument which shows that the very highest excited states of the model can not be doubly degenerate for s larger than some critical value. If these turn out to be true, the model shows an *eigenstate phase transition*, which means that up to some crititcal value of s along the PE line the full spectrum is doubly degenrate, and after that there will be always some states which do not have a partner with the opposite parity and the same energy. To address these questions, we are limited by finite size effect. A natural step would be using Density Matrix Renormalization Group(DMRG), which works very well in one dimension.

Other directions which we are considering to work on are finding the weak zero mode of the $\mathbb{Z}_3$ symmetric model and finding an analogue of PE line in the anyonic chains. Furthermore, it would be interesting to study these systems in higher dimensions, specially two dimensions.

Bibliography

[1] C.K. Chiu, J.C.Y. Teo, A.P. Schnyder, S. Ryu, Rev. Mod. Phys. **8**8, 035005 (2016).

[2] M. Z. Hasan, C. L. Kane, Rev. Mod. Phys. **8**2, 3045 (2010).

[3] "The Nobel Prize in Physics 2016 - Popular Information". Nobelprize.org. Nobel Media AB 2014. Web. 30 Oct 2017. `http://www.nobelprize.org/nobel_prizes/physics/laureates/2016/popular.html`

[4] "The Nobel Prize in Physics 2016 - Scientific background: Topological phase transitions and topological phases of matter". Nobelprize.org. Nobel Media AB 2014. Web. 30 Oct 2017.`http://www.nobelprize.org/nobel_prizes/physics/laureates/2016/advanced.html`

[5] H.E. Stanley,T.A. Kaplan, Phys. Rev. Lett. **1**7, 913 (1966)

[6] N.D. Mermin,H. Wagner, Phys. Rev. Lett. **1**7, 1133(1966)

[7] F. Wegner, Z. Phys **2**06, 465 (1967).

[8] M. Kardar, *Statistical physics of fields*, Cambridge University Press (2007).

[9] K. von Klitzing, G. Dorda, M. Pepper, Phys. Rev. Lett. **4**5, 494 (1980).

[10] D.J. Thouless,M. Kohmoto,M.P. Nightingale,M.den. Nijs, Phys. Rev. Lett. **4**9, 405 (1982).

[11] A.Y. Kitaev, Phys. Usp. **4**4, 131 (2001).

[12] V. Mourik, K. Zuo, S.M. Frolov, S.R. Plissard, E.P.A.M. Bakkers, L.P. Kouwenhoven, Science **3**36, 1003 (2012).

[13] M.T. Deng,C.L. Yu,G.Y. Huang,M. Larsson,P. Caroff,H.Q. Xu., Nano letters **1**2, 6414 (2012).

[14] S. Nadj-Perge, I.K. Drozdov, J. Li, H. Chen, S. Jeon, A.H. MacDonald, B.A. Bernevig, A. Yazdani, Science **3**46, 602 (2014).

[15] S. M. Albrecht,A.P. Higginbotham,M. Madsen, F. Kuemmeth,T.S. Jespersen,J. Nygrd,P. Krogstrup,C.M. Marcus, Nature **5**31, 206 (2016).

[16] A.Y. Kitaev, Ann. Phys. **3**03, 2 (2003).

[17] C. Nayak,S.H. Simon, A. Stern,M. Freedman,S.Das Sarma, Rev. Mod. Phys. **8**0, 1083(2008).

[18] J. Alicea,Y. Oreg,G. Refael,F.von Oppen,M.P.A. Fisher, Nature Phys.**7**, 412(2011).

[19] J. Alicea, P. Fendley, Annu. Rev. Condens. Matter Phys. **7** 11939 (2016).

[20] E. Lieb, T. Schultz, D. Mattis, Ann. Phys. **1**6, 407 (1961).

[21] P. Pfeuty, Ann. Phys. **5**7, 79 (1970).

[22] P. Fendley, J. Stat. Mech. P11020 (2012)

[23] G. Kells,D. Sen, J.K. Slingerland, S. Vishveshwara, Phys. Rev. B **8**9, 235130 (2014).

[24] P. Francesco, P. Mathieu, D. Sénéchal, *Conformal field theory*, Springer (2012).

[25] Y. Niu, S.B. Chung, C-H. Hsu, I. Mandal, S. Raghu, S. Chakravarty, Phys. Rev. B **8**5, 035110 (2012).

[26] D. Sticlet, C. Bena, P. Simon, Phys. Rev. B **8**7, 104509 (2013).

[27] S. Ryu, A.P. Schnyder, A. Furusaki, A.W.W. Ludwig New J. Phys. **1**2, 065010 (2010).

[28] A.M. Turner, F. Pollmann, E. Berg, Phys. Rev. B **8**3, 075102 (2011).

[29] L. Fidkowski, A. Kitaev, Phys. Rev. B **8**3, 075103 (2011).

[30] I. Peschel, V.J. Emery, Z. Phys. B **4**3, 241 (1981).

[31] H. Katsura, D. Schuricht, M. Takahashi, Phys. Rev. B **9**2, 115137 (2015).

[32] E. Sela, A. Altland,A. Rosch, Phys. Rev. B **8**4, 085114 (2011).

[33] P. Fendley, J. Phys. A: Math. Theor. **4**9, 30LT01 (2016).

[34] N. Moran, D. Pellegrino, J.K. Slingerland, G. Kells, Phys. Rev. B **9**5, 235127 (2017).

[35] J. Kurmann, H. Thomas, G. Müller, Physica A **1**12, 235 (1982).

[36] D. Sen, Phys. Rev. B **4**3, 5939 (1991).

[37] A. Dutta, D. sen, Phys. Rev. B **6**7, 094435 (2003).

[38] I. Affleck, T. Kennedy, E.H. Lieb, H. Tasaki, Phys. Rev. Lett. **5**9, 799 (1987).

[39] I. Affleck, T. Kennedy, E.H. Lieb, H. Tasaki, Commun. Math. Phys. **1**15, 477 (1988).

[40] J. Kemp, N.Y. Yao, C.R. Laumann, P. Fendley, J. Stat. Mech. 063105 (2017).

Accompanied Paper

Zero modes of the Kitaev chain with phase-gradients and longer range couplings

Iman Mahyaeh and Eddy Ardonne
Department of Physics, Stockholm University, SE-106 91 Stockholm, Sweden
(Dated: September 5, 2017)

We discuss the structure of the zero-modes of the Kitaev's one-dimensional p-wave superconductor, in the presence of both phase gradients and longer range pairing and hopping terms. As observed by Sticlet et al., one feature of such models is that for certain parameters, zero-modes can be present at one end of the system, while there are none on the other side. We explain the presence of this feature analytically, and show that it requires some fine-tuning of the parameters in the model. Thus as expected, these 'one-sided' zero-modes are neither protected by topology, nor by symmetry.

I. INTRODUCTION

A characteristic feature of many topological phases is the presence of gapless boundary modes. The (fractional) quantum Hall states are a prime example[1–3], and their boundary modes provide strong evidence of the topological nature of these states. Another prime example is the Kitaev chain, whose topological p-wave superconducting phase features so-called 'Majorana zero modes' at its boundary[4] Trying to establish the existence of the topological phase is often done by trying to establish the presence of the boundary modes. This has led to strong evidence for the topological phase in for instance strongly spin-orbit coupled nano-wires that are proximity coupled to an s-wave superconductor in the presence of a magnetic field[5–9], or in chains of magnetic ad-atoms[10–13]. It has been proposed that the zero energy Majorana bound states can be used as topologically protected q-bits, for quantum information processing purposes[14,15]. By now, there exist various proposals to manipulated these q-bits, either in T-junction systems, in which the Majorana bound states can be braided explicitly[16], or in Josephson coupled Kitaev chains, in which the coupling of the various chains allows operation on the q-bits[17].

Despite the intense research on the Kitaev chain models, there are still interesting features that deserve attention. In this paper, we look into one of them. It was observed by Sticlet et al.[18], that the zero-modes of Kitaev chains carrying a current, i.e., in the presence of a gradient in the phase of the order parameter, have interesting properties. The most striking feature is that is it possible that at one edge of the chain, there is pair of Majorana bound states (or better, one 'ordinary' Dirac zero mode), while there is no zero mode at the other end of the chain. Clearly, from a topological point of view, this means that the chain is in a trivial phase, but it is nevertheless worthwhile to investigate these zero-modes further. In this paper, we explain the presence of these zero-modes, via an exact solution of the zero modes of an extended Kitaev chain, i.e., in the presence of both complex and next nearest-neighbor hopping an pairing terms. We show that it is necessary to fine tune the couplings in order that these 'one-sided Dirac modes' to exist, but under these fine-tuned conditions, they can only disappear if the system undergoes a phase transition. Dropping the fine-tuning will gap out these zero modes immediately, leaving behind low-energy subgap modes. Apart from the analytical solution of the zero modes, we also present the solution of the full spectrum of the open Kitaev chain, for real, but otherwise arbitrary parameters, which does not seem to have appeared in the literature before.

The outline of the paper is as follows. We start in Sec. II by a brief review of the Lieb-Schultz-Mattis method to solve open quadratic fermionic systems, and focus on the case of complex couplings, which is essential for our purposes. In Sec. III, we provide the full solution of the open Kitaev chain, with real, but otherwise arbitrary couplings. In Sec. IV, we study the effect of next nearest-neighbor and complex couplings. Here, we focus entirely on the exact solutions for the zero-modes, and start by considering the effects of next nearest-neighbor couplings and complex pairings separately, before coming to the most interesting case, when both are present. In Sec. V, we discuss the result of the paper. Some details are delegated to the appendices.

II. THE LIEB-SCHULTZ-MATTIS METHOD

In this paper, we study the zero modes of Kitaev-like chains in the presence of longer range hopping and pairing terms. In particular, we are interested in the case where these couplings are complex. To study these systems, we use the method has been introduced by Lieb, Schultz and Mattis (LSM)[19] who used it, amongst other things, to solve the XY chain, for various types of boundary conditions. For a quadratic fermionic Hamiltonian with periodic boundary conditions (PBC), one diagonalizes the Hamiltonian by using a Fourier transformation, followed by a Bogoliubov transformation in the case of superconducting model. Without translational invariance one can still perform a Bogoliubov like transformation directly in real space. It was this method that LSM used to find the spectrum of the open XY chain (after using a Jordan-Wigner transformation to transform the spin degrees of freedom to polarized fermions).

In this section we review the LSM method and follow their notation for convenience. We consider two different cases. First, we look at the Hamiltonian with real

couplings and recall how one can derive the spectrum of the model analytically. Second, for a general quadratic Hamiltonian with complex couplings we present the equations governing the zero mode solutions, which we use throughout the paper.

Following LSM[19], we consider the general quadratic Hamiltonian of polarized fermions as follows,

$$H = \sum_{i,j=1}^{N} c_i^\dagger A_{ij} c_j + \frac{1}{2}(c_i^\dagger B_{ij} c_j^\dagger + h.c.), \tag{1}$$

in which c_i is a fermion annihilation operator on site i, A is a hermitian matrix, B is an antisymmetric matrix and N is the number of sites. Using a Bogoliubov like transformation, one can define new fermion operators, and diagonalize the Hamiltonian:

$$\eta_\alpha = \sum_{i=1}^{N} (g_{\alpha,i} c_i + h_{\alpha,i} c_i^\dagger), \tag{2}$$

$$H = \sum_{\alpha=1}^{N} \Lambda_\alpha \eta_\alpha^\dagger \eta_\alpha, \tag{3}$$

in which α labels the states and $g_{\alpha,i}$ and $h_{\alpha,i}$ are two functions, which are to be determined. This transformation is canonical, in the sense that new operators obey the fermionic anti-commutation relations, i.e. $\{\eta_\alpha, \eta_\beta^\dagger\} = \delta_{\alpha\beta}$.

Using the equation of motion, $[H, \eta_\alpha] = -\Lambda_\alpha \eta_\alpha$, one finds the equations for $g_{\alpha,i}$ and $h_{\alpha,i}$:

$$h_{\alpha,i} B_{ij}^* - g_{\alpha,i} A_{ij} = -\Lambda_\alpha g_{\alpha,j}, \tag{4}$$

$$h_{\alpha,i} A_{ij}^* - g_{\alpha,i} B_{ij} = -\Lambda_\alpha h_{\alpha,j}. \tag{5}$$

In order to find the full spectrum of the Hamiltonian, we now consider the case for which A and B have real elements. In this case, one defines new variables as

$$\phi_{\alpha,i} = g_{\alpha,i} + h_{\alpha,i}, \tag{6}$$

$$\psi_{\alpha,i} = g_{\alpha,i} - h_{\alpha,i}, \tag{7}$$

which we combine into row vectors, $\phi_\alpha = (\phi_{\alpha,1}, \ldots, \phi_{\alpha,N})$ and $\psi_\alpha = (\psi_{\alpha,1}, \ldots, \psi_{\alpha,N})$. Summing and subtracting Eqs.(4) and (5) gives two coupled equations for ϕ_α and ψ_α,

$$\phi_\alpha (A - B) = \Lambda_\alpha \psi_\alpha, \tag{8}$$

$$\psi_\alpha (A + B) = \Lambda_\alpha \phi_\alpha. \tag{9}$$

We note that the matrices act from the right side on the vectors. By acting with $A + B$ on Eq.(8) and $A - B$ on Eq.(9) from the right, the equations decouple

$$\phi_\alpha (A - B)(A + B) = \Lambda_\alpha^2 \phi_\alpha, \tag{10}$$

$$\psi_\alpha (A + B)(A - B) = \Lambda_\alpha^2 \psi_\alpha. \tag{11}$$

To find all the eigenvalues Λ_α and states η_α, one solves these two decoupled equations for ϕ_α and ψ_α. We explain how to do this in more detail in the next section for the *open* Kitaev chain[4] with real, but otherwise generic parameters.

It is well-known that fermionic systems can host Majorana zero modes on the edges of the system, which is a signature of the system being in a topological phase. In this paper, we study the zero modes of Hamiltonians with complex parameters, so we now allow the matrices A and B to be complex again. To distinguish a Majorana mode from the ordinary modes, we use stared labels, such as α^*. The Majorana modes satisfy $\eta_{\alpha^*} = \eta_{\alpha^*}^\dagger$. For a finite system, the energy of a Majorana mode is exponentially small in the system size; for instance in the case where we have a system with N sites the energy scales as $\Lambda_{\alpha^*} \sim e^{-\kappa N}$ with $\kappa > 0$[4,19]. Hence we are interested in finding general equations which allows one to find the corresponding states with zero energy, i.e. $\Lambda_{\alpha^*} = 0$, in the thermodynamic limit.

We thus search for a Majorana solution of Eqs.(4) and (5) with zero energy. Setting $h_{\alpha^*,i} = g_{\alpha^*,i}^*$ in Eqs. (4) and (5) gives:

$$g_{\alpha^*,i}^* B_{ij}^* = g_{\alpha^*,i} A_{ij}, \tag{12}$$

$$g_{\alpha^*,i}^* A_{ij}^* = g_{\alpha^*,i} B_{ij}, \tag{13}$$

By summing and subtracting these equations we get,

$$\mathrm{Re}[g(A - B)] = 0, \tag{14}$$

$$\mathrm{Im}[g(A + B)] = 0. \tag{15}$$

We use these equations to explore the wave functions ($g_{\alpha^*,i}$) of the zero modes in different cases in the following sections.

Before closing this section, we write the η operators in terms of Majorana operators for future reference. Using ϕ and ψ as defined above and defining Majorana operators as $\gamma_{A,j} = c_j^\dagger + c_j$ and $\gamma_{B,j} = i(c_j^\dagger - c_j)$, we write the fermion annihilation operator as follows

$$\eta_\alpha = \sum_{j=1}^{N} [\frac{\phi_{\alpha,j}}{2} \gamma_{A,j} + i \frac{\psi_{\alpha,j}}{2} \gamma_{B,j}]. \tag{16}$$

The algebra of Majorana operators can be calculated from the canonical anti-commutation relations of the c operators,

$$\{\gamma_{r,i}, \gamma_{r',j}\} = 2\delta_{rr'}\delta_{ij}. \tag{17}$$

Specifically, for the zero mode solution we can write the corresponding fermionic operator as follows:

$$\eta_{\alpha^*} = \sum_{j=1}^{N} (\mathrm{Re}[g_{\alpha^*,i}] \gamma_{A,j} - \mathrm{Im}[g_{\alpha^*,i}] \gamma_{B,j}). \tag{18}$$

III. THE SPECTRUM OF THE OPEN KITAEV CHAIN

In this section, we use the method of LMS to find the full spectrum of the Kitaev chain[4], for an open chain,

with real parameters, in particular we consider

$$H = \frac{1}{2}\sum_{j=1}^{N-1}(c_j^\dagger c_{j+1} + \Delta c_j^\dagger c_{j+1}^\dagger + h.c.) - \mu\sum_{j=1}^{N}(c_j^\dagger c_j - \frac{1}{2}) \ . \tag{19}$$

Here, μ denotes the chemical potential, Δ the strength of the pairing term, and we chose the hopping parameter $t = -1$[1]

Despite the fact that this model has been studied thoroughly, these results do not seem to have appeared in the literature, and we will use it to set the notation. Because we are interested in the zero-modes of more generic situations in the remainder of the paper, we also quickly review the nature of the zero-modes. These results are not new, but appeared in[19–21] and for generic parameters recently in[22].

It is well known[4] that the Kitaev chain is in a topological phase for $|\mu| < |t|$ and $\Delta \neq 0$. A profound feature of topological phase is the presence of a Majorana zero mode, that are exponentially localized near the edges of the system. In addition, the energy associated with this zero mode is exponentially small in the system size.

To set the scene, we follow Kitaev to show the presence of Majorana zero modes, by considering the special case of $\Delta = 1$ and $\mu = 0$. In this case, the Hamiltonian in terms of Majorana operators becomes,

$$H = -\frac{i}{2}\sum_{j=1}^{N-1}\gamma_{B,j}\gamma_{A,j+1}. \tag{20}$$

In this Hamiltonian, $\gamma_{A,1}$ and $\gamma_{B,N}$ are absent and therefore commute with it. So one can form a non-local fermionic state, $f_0 = \frac{1}{2}(\gamma_{A,1} + i\gamma_{B,N})$. The presence of this non-local fermionic mode is the characteristic feature of topological phase of the Kitaev chain. For $\Delta = -1$, unpaired Majorana operators would be $\gamma_{B,1}$ and $\gamma_{A,N}$, owing to the p-wave nature of pairing.

We leave this fine tuned point and consider arbitrary Δ, but keep $\mu = 0$ for the moment. This corresponds to the XY model, which was solved exactly by LSM for $|\Delta| < 1$, that is, the full spectrum including the wave functions were found[19]. For an open chain, there is a state with an exponentially small energy as a function of the system size. The wavefunction of this state is exponentially localized on the edges, namely $\phi_n \sim \left(\frac{1-|\Delta|}{1+|\Delta|}\right)^n$ where n denotes the position of the site measured from the left side of the chain. The associated ψ_n is localized on the right edge. Another fine tuned point that was studied previously corresponds to the TFIM, that is $t = -1$, $\Delta = \pm 1$ but arbitrary μ. Pfeuty showed that this model has a Majorana zero mode if $|\mu| < 1$. The associated wave function takes the form $\phi_n \sim |\mu|^n$ and is localized on the left edge of the system[20,21].

To find the Majorana zero modes for the general case, it is advantageous to first consider the model with periodic boundary conditions. That is, we need to consider the hopping and paring terms for the last site as well. We denoted the periodic Hamiltonian by $H_{PBC} = H + H_N$ where:

$$H_N = \frac{1}{2}(c_N^\dagger c_1 + \Delta c_N^\dagger c_1^\dagger + h.c.), \tag{21}$$

The solution of the periodic model is well known, and obtained by using a plane-wave ansatz for the wave functions (i.e., by Fourier-transforming the model). Using the method outlined in the previous section, we start by solving Eqs. (10) and (11) to find the spectrum. Since ϕ and ψ are related via Eqs. (8) and (9), we focus on ϕ. Writing Eq. (10) gives us one recursion relation:

$$\begin{aligned}&(1-\Delta^2)\phi_{\alpha,n-2} - 4\mu\phi_{\alpha,n-1} + [4\mu^2 + 2(1+\Delta^2)]\phi_{\alpha,n} \\ &+(1-\Delta^2)\phi_{\alpha,n+2} - 4\mu\phi_{\alpha,n+1} = 4\Lambda_\alpha^2\phi_{\alpha,n},\end{aligned} \tag{22}$$

where n denotes the sites and runs from 1 to N. Upon setting $\phi_{k,n} \sim e^{ikn}$, were we use the momentum k as a label, one finds the eigenvalues:

$$\Lambda_k^2 = (\mu - \cos k)^2 + \Delta^2 \sin^2 k, \qquad k = \frac{2\pi m}{N}, \tag{23}$$

where m runs over 0 to $N-1$.

We now consider the full spectrum of the open chain. Here, we merely give the results, and refer to the Appendix A, where the details of calculation are presented.

For the open chain we find the same recursion relation in the bulk which is valid for $3 \leq n \leq N-2$. However, we also have four boundary equations which should be treated separately (see Appendix A). We start by dealing with the bulk equations, using the method of LSM. That is, we use the same 'function' for the eigenvalues, though with a generic parameter α instead of the momentum k. To find the allowed values for the parameter α, one uses the 'boundary equations'. Hence we parametrize the eigenvalues as:

$$\Lambda_\alpha^2 = (\mu - \cos\alpha)^2 + \Delta^2 \sin^2\alpha, \tag{24}$$

and α is the label for the state. For the states, we use a power law ansatz, $\phi_{\alpha,n} \sim x_\alpha^n$, and we find four solutions, $x_\alpha = e^{\pm i\alpha}$ and $x_\alpha = e^{\pm i\beta}$ where

$$\cos\alpha + \cos\beta = \frac{2\mu}{1-\Delta^2}. \tag{25}$$

Note that α and β are not necessarily real, but the way we parametrize x_α turns out to be convenient. As described in the Appendix A, the relevant linear combination that

[1] The sign of t is irrelevant for the spectrum, but we set $t = -1$, because of the simpler relation with the associated XY model as studied in[19].

one uses to find a solution for the boundary equations is:

$$\begin{aligned}\phi_{\alpha,n} = A_1\Big\{ &\sin[(N+1)\beta]\sin(n\alpha) \\ &- \sin[(N+1)\alpha]\sin(n\beta)\Big\} \\ + A_2\Big\{ &\sin[(N+1)\beta]\sin[(N+1-n)\alpha] \\ &- \sin[(N+1)\alpha]\sin[(N+1-n)\beta]\Big\}. \end{aligned} \quad (26)$$

in which A_1 and A_2 are constants that are related via Eq. (A24). The boundary equations give rise to another constraint on α and β. This constraint can be shown to take the following form

$$\begin{aligned}&\sin^2\alpha + \sin^2\beta + \frac{1}{\Delta^2}(\cos\beta - \cos\alpha)^2 \\ &- 2\frac{\sin\alpha\sin\beta}{\sin[(N+1)\alpha]\sin[(N+1)\beta]} \\ &\times\{1 - \cos[(N+1)\alpha]\cos[(N+1)\beta]\} = 0. \end{aligned} \quad (27)$$

To obtain the full solution of the model, one needs to solve Eqs. (25) and (27) simultaneously. Though this can not be done analytically, it is straightforward to obtain the solutions numerically. Thus, we have characterized all the eigenvalues and eigenvectors $\phi_{\alpha,n}$ and by using Eq. (10), one finds $\psi_{\alpha,n}$.

Now we want to study these solutions and see when this model has a Majorana solution and what the corresponding wavefunction is. To find such solutions, we consider thermodynamic limit, i.e. $N \to \infty$, which makes the calculations easier.

We first mention that Δ can always set to be positive. One way to see this is by considering the transformation by which c_j goes to $e^{i\frac{\pi}{2}}c_j$. This transformation changes neither the hopping nor chemical potential term, but Δ changes to $-\Delta$. In addition solutions for $\mu < 0$ can be constructed from the solutions for $\mu > 0$. One can take the solution for $\mu > 0$, say $(\alpha, \beta) = (r, s)$. Now consider $(\alpha, \beta) = (r + \pi, s + \pi)$. This change gives a minus sign for the LHS of Eq. (25) as required, however it leaves Eq. (27) unchanged. Therefore, we restrict ourselves to $\Delta, \mu > 0$.

First we look at the solutions for large values of μ. In this case one can see that Eqs. (25) and (27) have N distinct real solutions for α, where we restrict α to lie in the range $0 < \alpha \leq \pi$ ($\alpha = 0$ gives $\phi_n = 0$; form more details, see Appendix A). However by decreasing chemical potential solution with the smallest value of α will 'disappear'. It is well known that for $\mu < 1$ one real solution is lost in the thermodynamic limit. For a finite chain this happens for $\mu < 1 + O(\frac{1}{N})$ where $O(\frac{1}{N})$ is a finite size correction. Thus, for $\mu < 1$ one must find an additional, complex solution. To find this solution, we consider three different cases.

1) $\Delta < 1$ *and* $\sqrt{1-\Delta^2} < \mu < 1$: In the thermodynamic limit one can check that the following solution satisfies Eqs.(25) and (27),

$$\alpha^* = i(\frac{1}{\xi_1} + \frac{1}{\xi_2}), \qquad \beta^* = i(\frac{1}{\xi_1} - \frac{1}{\xi_2}), \quad (28)$$

$$\cosh\frac{1}{\xi_1} = \frac{1}{\sqrt{1-\Delta^2}}, \quad \cosh\frac{1}{\xi_2} = \frac{\mu}{\sqrt{1-\Delta^2}}. \quad (29)$$

Furthermore it is straightforward to check that Eq.(24) gives $\Lambda_{\alpha^*} = 0$, hence the solution is indeed a zero mode. The wave function $\phi_{\alpha^*,n}$ for this zero mode is

$$\phi_{\alpha^*,n} = Ce^{-\frac{n}{\xi_1}}\sinh(\frac{n}{\xi_2}), \quad (30)$$

where C is a normalization constant. Moreover, it can be shown that based on structure of $A - B$ and $A + B$ matrices, one has $\psi_{\alpha^*,n} = \phi_{\alpha^*,N+1-n}$. From the fact that $\xi_1 < \xi_2$, it follows that ϕ_{α^*} is localized on the left edge while ψ_{α^*} is localized on right edge of the system. Hence we found two Majorana operators, that are located on the edges of the system, and the associated wavefunctions decay exponentially.

2) $\Delta < 1$ *and* $\mu < \sqrt{1-\Delta^2}$: In this range, one needs to use a different parametrization if one wants to use real parameters, as is evident from Eq.(29). This parametrization reads

$$\alpha^* = q + i\frac{1}{\xi}, \qquad \beta^* = q - i\frac{1}{\xi}, \quad (31)$$

$$\cos q = \frac{\mu}{\sqrt{1-\Delta^2}}, \quad \cosh\frac{1}{\xi} = \frac{1}{\sqrt{1-\Delta^2}}. \quad (32)$$

Basically we changed one of the characteristic length scales to become a wave vector. As in the previous case, this solution is indeed a zero mode, i.e. $\Lambda_{\alpha^*} = 0$, whose wavefunction is given by:

$$\phi_{\alpha^*,n} = Ce^{-\frac{n}{\xi}}\sin(nq). \quad (33)$$

This result indicates that ϕ (ψ) is localized on the left (right) edge with an oscillatory decaying wave function. We should point out that this result was obtained earlier by[22]. In addition, it was observed that the correlation functions in the model with PBC are oscillatory in the same regime, i.e., for $\mu < \sqrt{1-\Delta^2}$ with $\Delta < 1$, see for instance Refs. 23–25.

3) $\Delta > 1$: For this regime $\sqrt{1-\Delta^2}$ is imaginary, hence the previous solutions are not applicable. The new root can be written as

$$\alpha^* = i(\frac{1}{\xi_1} - \frac{1}{\xi_2}), \qquad \beta^* = \pi + i(\frac{1}{\xi_1} + \frac{1}{\xi_2}), \quad (34)$$

$$\sinh\frac{1}{\xi_1} = \frac{1}{\sqrt{\Delta^2-1}}, \quad \sinh\frac{1}{\xi_2} = \frac{\mu}{\sqrt{\Delta^2-1}}. \quad (35)$$

One can check that this solution represents a zero mode with the wave function:

$$\phi_{\alpha^*,n} = Ce^{-\frac{n}{\xi_1}} \times \begin{cases} \cosh(\frac{n}{\xi_2}), & \text{if } n \text{ is odd,} \\ \sinh(\frac{n}{\xi_2}) & \text{if } n \text{ is even.} \end{cases} \quad (36)$$

For this solution $\xi_1 < \xi_2$ since $\mu < 1$ and this guarantees that ϕ (ψ) is localized on the left (right) edge.

IV. ZERO-MODES FOR NEXT NEAREST-NEIGHBOUR AND COMPLEX COUPLINGS

In this section we study the zero modes in the presence complex hopping and pairing terms, both in the case with nearest neighbor hopping and pairing terms, as well as next-nearest neighbor (NNN) hopping and paring terms. The complex amplitudes model the presence of a phase gradient in the system.

In their fermionic incarnation, these generalized Kitaev models were studied in Refs. 18,26. In the language of spin models, adding NNN terms gives rise to so-called (one-dimensional) cluster models[26–30], but we concentrate ourselves on the fermionic version of these models.

An important feature of these models is the possibility of having more than one zero modes at each end, which is possible due to the presence of longer range terms. This can also be understood in terms of the classification of topological insulators and superconductors[31,32]. The Kitaev chain with real coupling constants belongs to class BDI for which the different topological phases can be labeled by the elements of $\mathbb{Z}$, in the absence of interactions. Adding interaction changes this picture such that new classification given by $\mathbb{Z}_8$ instead[33]. In the case with only nearest neighbor hopping and pairing terms, the model describes phases with at most one Majorana mode at each end of the system. However by adding NNN terms one finds phases with two Majorana modes at each end. This means that there would be two distinct topological phases with one and two zero modes solutions (in addition to the trivial phase, which does not have a zero mode).

Proposals for using the non-local fermionic state as a qubit, requires the ability to move Majorana edge states and even to do braiding. One proposal to achieve this is by inducing a phase gradient in the superconductor order parameter, i.e $\Delta_j = \Delta e^{i\theta_j}$, with non-uniform θ_j[34]. Having a complex superconductor order parameter breaks the time reversal symmetry in which case the model belongs to class D. For class D, we have the $\mathbb{Z}_2$ classification which means that the system could be either in the topological phase with at most one Majorana zero mode at each end, or in the trivial phase. Surprisingly, Sticlet et al. showed that NNN terms with a phase gradient can exhibit an exponentially localized fermionic zero mode on one edge[18]. Such a phase, though it is not topologically protected, has local zero modes. In Ref. 18 these models were investigated numerically. Here we present an analytical solution and study the zero-modes in detail. We first we review the Kitaev chain with NNN terms. After that, we study the effect of a constant phase gradient in the Kitaev chain. Finally, we combine the two complications and consider NNN terms and a phase gradient simultaneously.

A. Next nearest-neighbor couplings

In this section we consider the Kitaev chain and add NNN hopping and pairing terms. We start with the case for which all the parameters are real, hence the Hamiltonian belongs to class BDI. Setting $\mu = 1$, the problem has four energy scales, corresponding to the two hopping and two pairing amplitudes. To simplify the calculation we set the NN hopping and pairing terms equal to each other and we do the same for the NNN terms. Sticlet et al. studied this model under the same assumptions[18]. We will consider the model with arbitrary complex parameters in section IV D.

Thus, the Hamiltonian reads,

$$H = \frac{t}{2}\sum_{j=1}^{N-1}(c_j^\dagger c_{j+1} + c_j^\dagger c_{j+1}^\dagger + h.c.) - \mu\sum_{j=1}^{N}(c_j^\dagger c_j - \frac{1}{2}) + \frac{\lambda}{2}\sum_{j=1}^{N-2}(c_j^\dagger c_{j+2} + c_j^\dagger c_{j+2}^\dagger + h.c.) \quad (37)$$

where λ is the NNN hopping and pairing amplitude. To obtain the phase diagram and the functional form of Λ_α we first consider the model with periodic boundary conditions[18,26]. We do a Fourier transformation, $c_j = \frac{1}{\sqrt{N}}\sum_k e^{ikj}c_k$, and define $\Psi_k = (c_k, c_{-k}^\dagger)^{\mathrm{T}}$ to write the hamiltonian as

$$H = \frac{1}{2}\sum_k \Psi_k^\dagger \mathcal{H}_k \Psi_k,$$
$$\mathcal{H}_k = [-t\sin(k) - \lambda\sin(2k)]\tau^y + [t\cos(k) + \lambda\cos(2k) - \mu]\tau^z, \quad (38)$$

where the τ^α are Pauli matrices that act in the Nambu space Ψ_k. The Hamiltonian can be written as $\mathcal{H}_k = \mathbf{h}(k)\cdot\boldsymbol{\tau}$. One can find the phase diagram by calculating the winding number for $\mathbf{h}(k)$[18,32] or by looking at gap closing lines[26]. The phase diagram is presented in Fig. 1. The gap closes along the lines $\lambda = \mu + t$, $\lambda = \mu - t$ and $\lambda = -\mu$ for $|t| < 2|\mu|$. Note that in the figure we used $\mu = 1$.

Before looking at the zero mode solution(s) of an open chain, we first consider some limiting cases to understand the phase diagram. For very small $|t|, |\lambda| \ll |\mu|$ we get the trivial phase. The "0" in Fig. 1 indicates that there are no Majorana zero modes in this part of the phase diagram. Outside of the trivial region on the vertical axis where $t = 0$ we have two decoupled Kitaev chains, hence there are two zero modes at each end. For a fixed λ, adding NN terms couples these two chains. The two zero modes survive until the gap closes, thereafter there will only be one zero-mode at each end. The horizontal

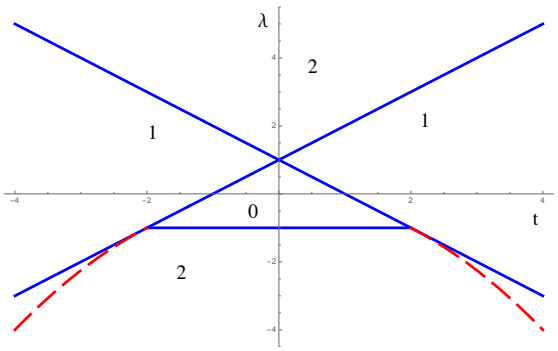

FIG. 1: Phase diagram for Kitaev chain with NNN terms, Eq. (37) for $\mu = 1$. The numbers in the plot show the number of Majorana zero modes at each end of the chain. The meaning of the red, dashed lines is explained in the main text.

axis with $\lambda = 0$ (i.e., the original Kitaev chain) belongs to this later region which is indicated by "1" in the Fig. 1.

To find the wave functions of the zero modes, we use Eqs. (8) and (9) with $\Lambda_\alpha = 0$. From Eq. (16) we see that if η_α is a Majorana mode (i.e., $\eta_\alpha^\dagger = \eta_\alpha$), ψ has to be purely imaginary. So for convenience we define $\psi = i\tilde{\psi}$ and we get $g = \frac{1}{2}(\phi + i\tilde{\psi})$. We use this convention from now on. We obtain the following 'bulk' equations

$$-\mu\phi_n + t\phi_{n+1} + \lambda\phi_{n+2} = 0 \tag{39}$$

$$\lambda\tilde{\psi}_{n-2} + t\tilde{\psi}_{n-1} - \mu\tilde{\psi}_n = 0\ . \tag{40}$$

The 'boundary' equations are $-\mu\phi_{N-1} + t\phi_N = 0$, $-\mu\phi_N = 0$, $-\mu\tilde{\psi}_1 = 0$ and $t\tilde{\psi}_1 - \mu\tilde{\psi}_2 = 0$. So we can use the ansatz $\phi_n \sim x_0^n$ and $\tilde{\psi}_n \sim x_0^n$, which gives the result

$$\begin{aligned}
\phi_n &= L_+ x_{0,+}^n + L_- x_{0,-}^n, \\
\tilde{\psi}_n &= R_+ x_{0,+}^{N-n+1} + R_- x_{0,-}^{N-n+1}, \\
x_{0,\pm} &= \frac{-t \pm \sqrt{t^2 + 4\lambda\mu}}{2\lambda},
\end{aligned} \tag{41}$$

where $L_\pm$ and $R_\pm$ are real normalization constants (the subscript "0" in the length scales indicates that we deal with a zero phase gradient).

We can extract the phase diagram from this result[26] and we set $\mu = 1$ to be able to compare with Fig. 1. For regions where $\lambda > 1 + |t|$ or both $\lambda < 1 - |t|$ and $\lambda < -1$ (corresponding to the upper and lower regions of Fig. 1), one can see that $|x_{0,\pm}| < 1$. This means that in these regions that are indicated by "2" the system has two independent zero mode solutions. In the right part of the phase diagram where $1 - t < \lambda < 1 + t$, there only exists one zero mode since $|x_{0,+}| < 1$ and $|x_{0,-}| > 1$. If $1 + t < \lambda < 1 - t$ we also have one zero mode, however, in this case $|x_{0,-}| < 1$ and $|x_{0,+}| > 1$. We note that in these regions, the boundary equations are also satisfied in the large N limit.

It is also interesting to note that for $t^2 + 4\lambda > 0$ the roots are real. Still they could be negative in some regions which gives rise to an oscillatory behavior of the wave functions, which are then proportional to $(-1)^n$. For $t^2 + 4\lambda < 0$ the roots become complex. The red, dashed lines in Fig. 1 specify the upper boundaries of this region (in the case $\lambda < -1$). In this case $|x_\pm| = \frac{1}{\sqrt{|\lambda|}}$ which gives us the the criterion $\lambda < -1$ in order to have a zero mode (in the region $t^2 + 4\lambda < 0$). In this part of phase diagram the correlation length only depends on λ, while the NN coupling t only affects the oscillatory part of the wave function.

Before moving to the case with both NNN terms as well as with a phase gradient, we first study the Kitaev chain with just a constant phase gradient.

B. Phase gradient in the order parameter

In this subsection, we consider the Kitaev chain, but with a phase gradient in the superconducting order parameter. With a super current in superconductor, the pairing term has a site dependent phase $\Delta_j = e^{ij\nabla\theta}$ where $\nabla\theta$ is the constant phase gradient, while j indicates the position of the site. In this case, the Hamiltonian reads

$$H = \frac{1}{2}\sum_{j=1}^{N-1}(c_j^\dagger c_{j+1} + e^{ij\nabla\theta} c_j^\dagger c_{j+1}^\dagger + h.c.) - \mu\sum_{j=1}^{N}(c_j^\dagger c_j - \frac{1}{2}). \tag{42}$$

This Hamiltonian belongs to class D. As we indicated above, the topological phases are labeled by elements of $\mathbb{Z}_2$, which means that the system could be in the topological phase with one Majorana zero mode at each end. Changing the gauge, we transform the fermionic operators as $c_j \to e^{ij\frac{\nabla\theta}{2}} c_j$. This transformation gives us site-independent couplings, but now also the hopping parameter has become complex. The transformed Hamiltonian is

$$\begin{aligned}
H = &\frac{1}{2}\sum_{j=1}^{N-1}(e^{i\frac{\nabla\theta}{2}} c_j^\dagger c_{j+1} + e^{-i\frac{\nabla\theta}{2}} c_j^\dagger c_{j+1}^\dagger + h.c.) \\
&- \mu\sum_{j=1}^{N}(c_j^\dagger c_j - \frac{1}{2}).
\end{aligned} \tag{43}$$

To find zero mode solution we use Eqs. (14) and 15. Details of the solution for the Majorana operator are given in Appendix B. The left Majorana solution is

$$\gamma_L = L\sum_{n=1}^{n=N}\left[\frac{\mu}{\cos(\frac{\nabla\theta}{2})}\right]^n \gamma_{A,n}, \tag{44}$$

where L is the normalization constant to make $\gamma_L^2 = 1$. This Majorana mode is located at the left side of the system, and is a solution in the large N limit. The right

Majorana mode is more complicated,

$$\gamma_R = R\sum_{n=1}^{n=N}\Big[\frac{\mu}{\cos(\frac{\nabla\theta}{2})}\Big]^{N-n+1}\times \\ [\sin(\frac{\nabla\theta}{2})\gamma_{A,n}+\cos(\frac{\nabla\theta}{2})\gamma_{B,n}], \quad (45)$$

where R is the normalization constant to make $\gamma_R^2=1$. Using the Majorana modes γ_L and γ_R, one can construct one fermionic mode $f_0=1/2(\gamma_L+i\gamma_R)$ as usual. We note that to have a localized zero mode we have the criteria $|\mu|<|\cos(\frac{\nabla\theta}{2})|$. This means that turing on the phase gradient shrinks the topological region. Second, we see that the left Majorana consists only of γ_A Majorana operators (recall the definition above Eq. (16)), however, the right one involves both γ_B's as well as γ_A's. In the case that $\nabla\theta=0$ the left Majorana mode only involves γ_A operators and the right Majorana modes only γ_B operators. This feature of the solution comes from the fact that for real A and B matrices (see Eqs. (14) and 15), the equations governing ϕ and $\tilde{\psi}$ are decoupled - recall that $g=\frac{1}{2}(\phi+i\tilde{\psi})$. Adding the phase gradient makes these matrices complex, hence the equations become coupled and the solutions become more complicated. The direction of the phase gradient shows itself in the elements of the A and B matrices and gives rise to this asymmetry; the "left-right" symmetry is broken explicitly.

In the next section we add NNN terms to the current problem[18]. The results presented in the current subsection are useful to understand zero mode solution(s) when one adds the NNN terms.

C. Next nearest neighbor terms along with a phase gradient in the order parameter

We now consider NNN terms in the presence of a constant phase gradient. Again we set the hopping and pairing amplitudes equal to each other for both the nearest neighbors and NNN terms. Following Sticlet et al[18], the Hamiltonian reads,

$$H=\frac{t}{2}\sum_{j=1}^{N-1}(c_j^\dagger c_{j+1}+e^{ij\nabla\theta}c_j^\dagger c_{j+1}^\dagger+h.c.) \\ +\frac{\lambda}{2}\sum_{j=1}^{N-2}(c_j^\dagger c_{j+2}+e^{ij\nabla\theta}c_j^\dagger c_{j+2}^\dagger+h.c.) \\ -\mu\sum_{j=1}^{N}(c_j^\dagger c_j-\frac{1}{2}), \quad (46)$$

where we assumed the same phase dependence for the nearest neighbor and NNN pairing terms, with the same phase for both terms involving the first site. As we mentioned above, for $\nabla\theta=0$ this model has a trivial phase without any zero mode and two topological phases that hosts one or two Majorana zero modes respectively (see Fig. 1). For $\nabla\theta\neq 0$, the model belongs to class D. This means that, contrary to $\nabla\theta=0$ case, there is only one type of topological phase. The phase that had two Majorana zero modes becomes trivial upon adding the phase gradient. The natural question it then what happens to the phases with two Majorana edge states? Despite the fact that the phase has become trivial, one finds that it is still an interesting trivial phase, as was already observed in 18. Here, we study the zero modes of the model, and shed light on the zero mode present in one of the trivial phases.

By transforming $c_j\to e^{ij\frac{\nabla\theta}{2}}c_j$ as in the previous section, the Hamiltonian becomes

$$H=\frac{t}{2}\sum_{j=1}^{N-1}(e^{i\frac{\nabla\theta}{2}}c_j^\dagger c_{j+1}+e^{-i\frac{\nabla\theta}{2}}c_j^\dagger c_{j+1}^\dagger+h.c.) \\ +\frac{\lambda}{2}\sum_{j=1}^{N-2}(e^{i\nabla\theta}c_j^\dagger c_{j+2}+e^{-i\nabla\theta}c_j^\dagger c_{j+2}^\dagger+h.c.) \\ -\mu\sum_{j=1}^{N}(c_j^\dagger c_j-\frac{1}{2}). \quad (47)$$

As we show in the next section (where we consider the model for general parameters), locations of the phase transitions of this model is very similar to the locations of the phase transitions of the model with zero phase gradient, $\nabla\theta=0$. Namely, the phase boundaries are the same, if written in terms of the variables $\tilde{t}=\cos(\nabla\theta/2)t$ and $\tilde{\lambda}=\cos(\nabla\theta)\lambda$, while μ remains unchanged. So, the gap closes when $\tilde{\lambda}=\mu\pm\tilde{t}$, as well as when both $\tilde{\lambda}=-\mu$ and $|\tilde{t}|\leq 2|\mu|$.

Sticlet et al.[18] showed that the topological phase of this model has one zero mode at both edges as expected. The trivial phase, however, is divided in two regions. One trivial phase does not have any zero mode, while the other trivial phase has two 'Majorana' zero modes that are localized on one edge (i.e., a localized fermionic zero mode), while there is no zero mode on the other edge. The former trivial phase corresponds to the trivial phase of the model without phase gradient while the later trivial phase corresponds to the topological phase of the model without phase gradient with two Majorana zero modes. In what follows we present analytical wave functions for all the zero modes and determine for which parameters they are present. To find the Majorana zero modes we use Eqs. (14) and 15 and as before, we set $g_n=\frac{1}{2}(\phi_n+i\tilde{\psi}_n)$. The 'bulk equations' read

$$-\mu\tilde{\psi}_n+t\cos(\frac{\nabla\theta}{2})\tilde{\psi}_{n-1}+\lambda\cos(\nabla\theta)\tilde{\psi}_{n-2}=0, \quad (48)$$

$$-\mu\phi_n+t\cos(\frac{\nabla\theta}{2})\phi_{n+1}+\lambda\cos(\nabla\theta)\phi_{n+2}= \\ t\sin(\frac{\nabla\theta}{2})\Big(\tilde{\psi}_{n-1}-\tilde{\psi}_{n+1}\Big)+\lambda\sin(\nabla\theta)\Big(\tilde{\psi}_{n-2}-\tilde{\psi}_{n+2}\Big). \quad (49)$$

In this case, there are four boundary equations (two for each end) that differ from the bulk ones, namely

$$-\mu\tilde{\psi}_1 = 0 \qquad t\cos(\frac{\nabla\theta}{2})\tilde{\psi}_1 - \mu\tilde{\psi}_2 = 0 \tag{50}$$

and

$$\begin{aligned} &-\mu\phi_{N-1} + t\cos(\frac{\nabla\theta}{2})\phi_N = \\ &t\sin(\frac{\nabla\theta}{2})(\tilde{\psi}_{N-2} - \tilde{\psi}_N) + \lambda\sin(\nabla\theta)\tilde{\psi}_{N-3} \\ &-\mu\phi_N = t\sin(\frac{\nabla\theta}{2})\tilde{\psi}_{N-1} + \lambda\sin(\nabla\theta)\tilde{\psi}_{N-2}\ . \end{aligned} \tag{51}$$

We start by solving the bulk equations, without paying attention to the boundary equations. We then solve the boundary equations, in the different regimes of the phase diagram.

The equations for ϕ_n involves the solution for ψ_n. Thus, the solution for ϕ_n consists of two pieces, namely the general solution to Eq. (49) with the right hand side set to zero, which we will denote by $\phi_{\mathrm{gen},n}$, as well as a specific solution, for the full equation. We start the ansatz $\phi_{\mathrm{gen},n} = x^n$. This gives us two correlation length scales

$$x_\pm = \frac{-t\cos(\frac{\nabla\theta}{2}) \pm \sqrt{t^2\cos^2(\frac{\nabla\theta}{2}) + 4\lambda\mu\cos(\nabla\theta)}}{2\lambda\cos(\nabla\theta)}\ . \tag{52}$$

Thus, the generic solution is $\phi_{\mathrm{gen},n} = L_+x_+^n + L_-x_-^n$, where $L_\pm$ are constants. As before, $\tilde{\psi}_n = \phi_{\mathrm{gen},N-n+1}$, which shows that the generic solution for ϕ is localized on the left edge and the solution for $\tilde{\psi}$ is localized on the right edge, $\tilde{\psi} = R_+x_+^{N-n+1} + R_-x_-^{N-n+1}$, with $R_\pm$ two constants. To find the full solution ϕ_n, based on Eq.(49) we need to add a particular solution to $\phi_{\mathrm{gen},n}$ of the form $S_+x_+^{N-n+1} + S_-x_-^{N-n+1}$ with constant $S_\pm = \kappa_\pm R_\pm$, since it should behave as $\tilde{\psi}$. After some algebra, one finds that

$$\kappa_\pm = -\tan(\nabla\theta) + \frac{t\sin(\frac{\nabla\theta}{2})}{\cos(\nabla\theta)\Big[\mu + \lambda\cos(\nabla\theta)\Big]}x_\pm\ . \tag{53}$$

The general solution to the bulk equations (48) and (49) is thus given by

$$\begin{aligned} &\tilde{\psi}_n = R_+x_+^{N-n+1} + R_-x_-^{N-n+1}, \\ &\phi_n = L_+x_+^n + L_-x_-^n + S_+x_+^{N-n+1} + S_-x_-^{N-n+1}, \\ &S_\pm = \kappa_\pm R_\pm, \end{aligned} \tag{54}$$

With the general solution for the bulk equations at hand, we turn our attention to the boundary equations, which we solve in the different regimes.

1) $|x_\pm| > 1$: In this case, both characteristic length scales are bigger than one, which occurs for the part of the phase diagram where the model without phase gradient is in the trivial phase. In this case, it is not hard to convince oneself that the boundary equations (50) and (50) lead to $L_\pm = R_\pm = 0$, which means that, as expected, there are no zero modes in this regime.

2) $|x_+| < 1$ *and* $|x_-| > 1$: In this case, the model is topological, and corresponds to the phase with parameters $0 < \tilde{t} \gg \tilde{\lambda}$. In this regime, x_-^n increase with n, which means that x^n is localized on the right edge instead of the left one. It is therefore convenient to write this solutions as $\tilde{L}_-(\frac{1}{x_-})^{N-n+1}$, with $\tilde{L}_- = x_-^{N+1}L_-$, to highlight that this solution is localized on the right edge.

The boundary equations (50) imply that $R_- = S_- = 0$. The boundary equations (51) give, after some algebra, that $\tilde{L}_- = -R_+\frac{t\sin(\nabla\theta/2)}{\cos(\nabla\theta)(\mu+\lambda\cos(\nabla\theta))}$, while $S_+ = \kappa_+R_+$ as before. Thus, the solution for the zero mode is given by

$$\tilde{\psi}_n = R_+x_+^{N-n+1}\ , \tag{55}$$

$$\phi_n = L_+x_+^n + S_+x_+^{N-n+1} + \tilde{L}_-(\frac{1}{x_-})^{N-n+1}\ . \tag{56}$$

We find that in this case, there is one zero mode, that is localized on both edges of the system. One special property of this zero mode, which differs from the case without a phase gradient, is that ϕ_n has support on both edges of the system, while ψ_n only has support on the right edge. Finally, we note that the case $|x_+| > 1$ and $|x_-| < 1$ is completely analogous.

3) $|x_\pm| < 1$: This case corresponds to the part of the phase diagram in which the model without phase gradient has two zero modes on both side of the system. With the phase gradient, this model is in a trivial phase. To determine if there are any zero modes, we again solve the boundary equations. The boundary equations for $n = 1, 2$, i.e. (50), give rise to terms that are proportional to $\tilde{\psi}$ at the left edge. Eq.(54) assures that these terms are of order $x_\pm^N$ and can be neglected in the thermodynamic limit. So the solution satisfies the boundary equations (50). The boundary equations (51) do give a non-trivial constraint. Namely, for a non-zero phase gradient $\nabla\theta \neq 0$ (for $\nabla\theta = 0$ the boundary equations are satisfied), one finds that

$$R_+x_+ + R_-x_- = 0 \qquad R_+x_+^2 + R_-x_-^2 = 0. \tag{57}$$

These two boundary equations imply that $R_\pm = 0$. We conclude that in this regime there are two zero modes on the left side of the system, and none on the right side, i.e. $\phi_n = L_+x_+^n + L_-x_-^n$ and $\tilde{\psi}_n = 0$. This precisely corresponds to the surprising result obtained by Sticlet et al[18]. We stress that this ordinary, or 'Dirac' zero mode on the left side of the system is not topological, but is in fact a consequence of fine tuning the parameters. We discuss this fine tuning in more detail in Section IV D. Nevertheless, as long as one keeps these parameters fine tuned, the only way this localized zero mode can disappear is via a phase transition to one of the other phases present in the model. Upon going away from the fine-tuned point,

this Dirac zero mode gaps out, leaving behind a fermionic mode at finite energy.

We close this section by mentioning that it is of course possible to have the localized Dirac zero mode at the other edge of the system. One way is by changing the phase dependence of the original pairing terms in the original Hamiltonian Eq. (46) to $\frac{t}{2}e^{i(j+1)\nabla\theta}c_j^\dagger c_{j+1}^\dagger + \frac{\lambda}{2}e^{i(j+2)\nabla\theta}c_j^\dagger c_{j+2}^\dagger$. Basically the same calculation shows that this pairing leads to two zero modes on right and none on the left side. The model with these pairing terms has the same topological and trivial phases, however the left and right sides of the chain change their role. We note that merely changing $\nabla\theta \to -\nabla\theta$ does not change the role of the left and right hand side of the system. As we show in the next subsection, in the translational invariant formulation of the model, as in Eq. (47), the location of the zero-modes is determined by the relative sign of the phases of the hopping and paring terms.

D. The general case

To understand the fine tuning that is necessary to have the Dirac zero mode that resides on one side of the system as described in the previous section, we look at the more general Hamiltonian,

$$\begin{aligned} H = &\frac{1}{2}\sum_{j=1}^{N-1}(t_1 c_j^\dagger c_{j+1} + \Delta_1 c_j^\dagger c_{j+1}^\dagger + h.c.) \\ &+ \frac{1}{2}\sum_{j=1}^{N-2}(t_2 c_j^\dagger c_{j+2} + \Delta_2 c_j^\dagger c_{j+2}^\dagger + h.c.) \\ &- \mu\sum_{j=1}^{N}(c_j^\dagger c_j - \frac{1}{2}), \end{aligned} \tag{58}$$

where t_1, Δ_1, t_2 and Δ_2 are arbitrary complex parameters. In the case of periodic boundary conditions, we can define $\Psi_k = (c_k, c_{-k}^\dagger)^{\mathrm{T}}$ and write the Hamiltonian as:

$$\begin{aligned} H &= \frac{1}{2}\sum_k \Psi_k^\dagger \mathcal{H}_k \Psi_k,\ \mathcal{H}_k = h_0(k)\mathbf{1} + \mathbf{h}(k).\boldsymbol{\tau}, \\ h_0(k) &= -\Im(t_1)\sin k - \Im(t_2)\sin(2k), \\ h_1(k) &= -\Im(\Delta_1)\sin k - \Im(\Delta_2)\sin(2k), \\ h_2(k) &= -\Re(\Delta_1)\sin k - \Re(\Delta_2)\sin(2k), \\ h_3(k) &= \Re(t_1)\cos k + \Re(t_2)\cos(2k) - \mu, \end{aligned} \tag{59}$$

where $\mathbf{1}$ is the two by two identity matrix. Performing a unitary transformation with $U = \frac{1}{\sqrt{2}}(\tau^x + \tau^z)$ we get,

$$\mathcal{Q}_k = U^\dagger \mathcal{H}_k U = \begin{pmatrix} h_0(k)+h_1(k) & h_3(k)+ih_2(k) \\ h_3(k)-ih_2(k) & h_0(k)-h_1(k) \end{pmatrix}. \tag{60}$$

By comparing the model we discuss here, Eq. (47) with (59) we find that in this case, all the imaginary parts depends are proportional to $\sin(\nabla\theta/2)$ or $\sin(\nabla\theta)$, for the nearest neighbor or NNN case respectively. So, these terms vanish for $\nabla\theta = 0$. In that case, we obtain

$$\mathcal{Q}_k\big|_{\nabla\theta=0} = \begin{pmatrix} 0 & h_3(k)+ih_2(k) \\ h_3(k)-ih_2(k) & 0 \end{pmatrix}. \tag{61}$$

Since we performed an unitary transformation, Det $\mathcal{Q}_k$ = Det $\mathcal{H}_k$. So in the gapped phase, either topological or trivial, $\mathrm{Det}\mathcal{Q}_k = |h_3(k) + ih_2(k)|^2 \neq 0$ can be used to define a topological invariant via the winding of $\mathrm{Arg}(h_3(k) + ih_2(k))$, see[32]. This calculation leads to the same phase diagram we discussed before, see Fig. 1.

We now consider a phase gradient, i.e. $\nabla\theta \neq 0$, which is the case we are interested in. Based on Eq. (47) we have

$$\begin{aligned} h_0(k) &= -t\sin(\frac{\nabla\theta}{2})\sin k - \lambda\sin(\nabla\theta)\sin(2k), \\ h_1(k) &= t\sin(\frac{\nabla\theta}{2})\sin k + \lambda\sin(\nabla\theta)\sin(2k), \\ h_2(k) &= -t\cos(\frac{\nabla\theta}{2})\sin k - \lambda\cos(\nabla\theta)\sin(2k), \\ h_3(k) &= t\cos(\frac{\nabla\theta}{2})\cos k + \lambda\cos(\nabla\theta)\cos(2k) - \mu. \end{aligned} \tag{62}$$

The fact that $\Im(t_1) + \Im(\Delta_1) = \Im(t_2) + \Im(\Delta_2) = 0$, gives rise to $\mathcal{Q}_{k,11} = 0$. This means that, similar to the $\nabla\theta = 0$ case, we have that $\mathrm{Det}\mathcal{Q}_k = |h_3(k)+ih_2(k)|^2$, despite the fact that $\mathcal{Q}_{k,22} \neq 0$.

Thus we find an *effective* same phase diagram for the model with the phase gradient, namely the one given in Fig. 1, if we replace $t \to t\cos(\frac{\nabla\theta}{2})$ and $\lambda \to \lambda\cos(\nabla\theta)$.

As we indicated in the previous section, by changing the paring terms in the original Hamiltonian Eq. (46) to $\frac{t}{2}e^{i(j+1)\nabla\theta}c_j^\dagger c_{j+1}^\dagger + \frac{\lambda}{2}e^{i(j+2)\nabla\theta}c_j^\dagger c_{j+2}^\dagger$, we can have the situation that the system has two 'Majorana' zero modes on the right edge and none on the left side. The gauge transformation $\tilde{c}_j = e^{ij\frac{\nabla\theta}{2}}c_j$ changes these terms to $\frac{t}{2}e^{i\frac{\nabla\theta}{2}}\tilde{c}_j^\dagger\tilde{c}_{j+1}^\dagger + \frac{\lambda}{2}e^{i\nabla\theta}\tilde{c}_j^\dagger\tilde{c}_{j+2}^\dagger$. The hopping terms $\frac{t}{2}c_j^\dagger c_{j+1} + \frac{\lambda}{2}c_j^\dagger c_{j+2}$ become $\frac{t}{2}e^{i\frac{\nabla\theta}{2}}\tilde{c}_j^\dagger\tilde{c}_{j+1} + \frac{\lambda}{2}e^{i\nabla\theta}\tilde{c}_j^\dagger\tilde{c}_{j+2}$ as before. In this case we find that $\Im(t_1) - \Im(\Delta_1) = \Im(t_2) - \Im(\Delta_2) = 0$, which results in $\mathcal{Q}_{k,22} = 0$.

In class BDI, all the information about the zero modes is encoded in $\mathrm{Det}\mathcal{Q}_k$ The discussion above shows that this is not so in the present case. Whether $\mathcal{Q}_{k,11} = 0$ or $\mathcal{Q}_{k,22} = 0$ plays an important role in determining the position of the (non-topological) localized zero modes. It is also clear what fine tuning we need in order to have a pair of 'Majorana' zero modes localized at one side of the system and none on the other. We need either $\mathcal{Q}_{k,11}$ or $\mathcal{Q}_{k,22}$ to be zero, but not both. This is the case if we fine tune $\Im(t_1 + \Delta_1) = \Im(t_2 + \Delta_2) = 0$ or $\Im(t_1 - \Delta_1) = \Im(t_2 - \Delta_2) = 0$, but not both which would imply that all these parameters are real, and one has an equal number of zero-modes on either side of the system.

To explore this situation further, we write the Hamil-

tonian in terms of Majorana operators,

$$\begin{aligned}
H = & \frac{\Im(t_1+\Delta_1)}{4}\sum_{j=1}^{N-1} i\gamma_{A,j}\gamma_{A,j+1} \\
& + \frac{\Re(t_1-\Delta_1)}{4}\sum_{j=1}^{N-1} i\gamma_{A,j}\gamma_{B,j+1} \\
& - \frac{\Re(t_1+\Delta_1)}{4}\sum_{j=1}^{N-1} i\gamma_{B,j}\gamma_{A,j+1} \\
& + \frac{\Im(t_1-\Delta_1)}{4}\sum_{j=1}^{N-1} i\gamma_{B,j}\gamma_{B,j+1} \\
& + \frac{\Im(t_2+\Delta_2)}{4}\sum_{j=1}^{N-2} i\gamma_{A,j}\gamma_{A,j+2} \\
& + \frac{\Re(t_2-\Delta_2)}{4}\sum_{j=1}^{N-2} i\gamma_{A,j}\gamma_{B,j+2} \\
& - \frac{\Re(t_2+\Delta_2)}{4}\sum_{j=1}^{N-2} i\gamma_{B,j}\gamma_{A,j+2} \\
& + \frac{\Im(t_2-\Delta_2)}{4}\sum_{j=1}^{N-2} i\gamma_{B,j}\gamma_{B,j+2} \\
& - \frac{\mu}{2}\sum_{j=1}^{N} i\gamma_{A,j}\gamma_{B,j}. \qquad (63)
\end{aligned}$$

As a simple example we can see that for Hamiltonian presented in Eq. (47), setting $\mu = 0$ and $\nabla\theta = \pi$, yields following Majorana representation

$$H = \frac{t}{2}\sum_{j=1}^{N-1} i\gamma_{B,j}\gamma_{B,j+1} + \frac{\lambda}{2}\sum_{j=1}^{N-2} i\gamma_{B,j}\gamma_{A,j+2}, \qquad (64)$$

where it is evident that $\gamma_{A,1}$ and $\gamma_{A,2}$ do not appear in the Hamiltonian and therefor commute with it. Hence there are two Majorana zero modes on the left edge.

It is interesting to note that for $\nabla\theta = \pi$, the Hamiltonian belongs to class BDI. From the form of the Hamiltonian in Eq. (47) this is not obvious, but it is for the form Eq. (46), because all the coupling constants are real. On the other hand, in this form, some of the couplings are staggered, and in the periodic case, the model is translationally invariant with a two-site unit cell. The phase diagram has a different structure in this case, with only three phases. The phase boundaries do not depend on t, and are given by $\lambda = \pm\mu$. Because of the two-site unit cell, we use the formulation of the phase-winding invariant as given by[35]. One finds that all three phases are in fact trivial. In the trivial phases with $|\lambda| > |\mu|$, there is a localized Dirac zero mode only on the left side of the system, and no zero modes on the right side. This is consistent with the analysis of the model based on the from Eq. (47). From the point $\nabla\theta = \pi$ it is clear that also in symmetry class BDI, there are Hamiltonians that have trivial phases, which have a localized Dirac zero mode only on one side of the system, if parameters are fine-tuned.

Our previous discussion led us to conclude that $\Im(t_1 + \Delta_1) = \Im(t_2 + \Delta_2) = 0$ could result in two zero modes on the left edge. Based on Eq. (63) we can see that this means that there should not be any terms like $i\gamma_{A,j}\gamma_{A,j+1}$ and $i\gamma_{A,j}\gamma_{A,j+2}$ in the Hamiltonian. We can shed more light on this issue based on our analytical solution for the non-uniform pairing with nearest neighbor hopping and pairing.

As a first a step, we assume that $t = 0$. This means that we have two decoupled chains with a phase gradient. Our previous analysis shows that in the topological phase we have one Majorana zero mode on each edge. The wavefunctions for these Majorana modes are given in Eqs. (44) and (45). The crucial difference between these two wave functions originates in the direction of the phase gradient, which causes the left mode to be independent of γ_B, while the right modes consists of both γ_A and γ_B. Namely, for the left mode g_n is purely real while for the right mode g_n is complex, and hence involves both ϕ and $\tilde{\psi}$.

In the second step, we turn on nearest neighbor couplings, i.e. $t \neq 0$. We see that the first four terms in the Hamiltonian Eq. (63) result in a coupling between the zero modes of the two decoupled chains. Under the assumption that $\Im(t_1 + \Delta_1) = 0$ and $\Im(t_2 + \Delta_2) = 0$, which holds in our analytic calculation of the zero modes, we find that the right zero modes from the two different chains become coupled because of the $i\gamma_{B,j}\gamma_{B,j+1}$ terms present then $t \neq 0$, which gaps them out. On the other hand, the zero modes on the left edge do not become coupled directly, and remain gapless. Their wavefunctions are modified to the new ones presented in Eq. (54).

Finally, we mention that we checked numerically that under the conditions $\Im(t_1 + \Delta_1) = \Im(t_2 + \Delta_2) = 0$, the system has two zero modes located on the left edge, if the parameters are such that the same system, but without a phase gradient, would have two zero modes on both edges. The same holds true in the case that $\Im(t_1 - \Delta_1) = \Im(t_2 - \Delta_2) = 0$, if one exchanges the left and right edge of the system.

V. DISCUSSION

In this paper, we investigated the 'one-sided' fermionic zero modes observed by Sticlet et al.[18], by solving the Kitaev model, in the presence of longer range and complex hopping and pairing terms for open chains. From our investigation, it became clear that fine-tuned parameters are necessary for such zero modes to exists, but under the fine-tuned conditions, a phase-transition is required in order to destroy them. Leaving the fine-tuned conditions gaps these zero-modes out, turning them into one-sided low-energy subgap modes. Phases with such one-sided

bound states can occur both in one-dimensional systems in class D, as well as in class BDI. These modes are not protected by topology, which means that they can occur in the topologically trivial phase.

The general condition for the existence of 'one-sided zero modes' is most easily explained in terms of the Majorana formulation of the chains. Starting from a situation in which two pairs of (delocalized) Majorana bound states are present (i.e., in class BDI), one needs a perturbing term such that the two Majoranas describing the mode on, say, the left side are coupled, while the modes on the right side are not.

There has been a lot of progress on models in higher dimensions, that exhibit exact zero modes, see for instance Ref. 36. It would be interesting to investigate if it is possible to construct models, that exhibit 'one-sided' zero modes along the lines of the ones described in this paper, even in those higher-dimensional systems.

Acknowledgements – We would like to thank F. Pollmann, C. Spånslätt and R. Verresen for interesting discussions. This research was sponsored, in part, by the Swedish research council.

Appendix A: Details of the Kitaev chain spectrum calculation

In this appendix we present details of the solution for the open Kitaev chain with generic real parameters and free boundary conditions. The Hamiltonian reads:

$$H = \frac{1}{2}\sum_{j=1}^{N-1}(c_j^\dagger c_{j+1} + h.c) + \frac{\Delta}{2}\sum_{j=1}^{N-1}(c_j^\dagger c_{j+1}^\dagger + h.c) - \mu\sum_{j=1}^{N}(c_j^\dagger c_j - \frac{1}{2}). \tag{A1}$$

It is helpful to recall the (of course well known) solution for the periodic case, which is obtained via a Fourier transformation, $c_j = \frac{1}{\sqrt{N}}\sum_k e^{ikj}c_k$, and defining $\Psi_k = (c_k, c_{-k}^\dagger)^{\mathrm{T}}$. This results in

$$H = \frac{1}{2}\sum_k \Psi_k^\dagger \begin{pmatrix} -\mu+\cos k & i\Delta\sin k \\ -i\Delta\sin k & \mu-\cos k \end{pmatrix}\Psi_k. \tag{A2}$$

Diagonalization of this 2×2 matrix gives us:

$$H = \sum_k \epsilon_k(f_k^\dagger f_k - \frac{1}{2}), \tag{A3}$$

$$\epsilon_k = \sqrt{(\mu-\cos k)^2 + \Delta^2\sin^2 k}, \tag{A4}$$

where f_k is a new fermionic quasiparticle annihilation operator.

To tackle the open case, we use the method which is reviewed in Sec. II. To this end, we need to arrange the Hamiltonian to have the form of Eq. (1),

$$H = \sum_{i,j=1}^{N} c_i^\dagger A_{ij} c_j + \frac{1}{2}(c_i^\dagger B_{ij} c_j^\dagger + h.c.). \tag{A5}$$

To find ϕ_α and ψ_α from Eqs. (10) and (11) i.e.,

$$\begin{aligned} \phi_\alpha(A-B)(A+B) &= \Lambda_\alpha^2\phi_\alpha \\ \psi_\alpha(A+B)(A-B) &= \Lambda_\alpha^2\psi_\alpha\ , \end{aligned}$$

we have to construct the matrices $A-B$ and $A+B$.

We present these matrices for the more general case of Hamiltonian in Eq. (58), i.e.,

$$H = \frac{1}{2}\sum_{j=1}^{N-1}(t_1 c_j^\dagger c_{j+1} + \Delta_1 c_j^\dagger c_{j+1}^\dagger + h.c.) + \frac{1}{2}\sum_{j=1}^{N-2}(t_2 c_j^\dagger c_{j+2} + \Delta_2 c_j^\dagger c_{j+2}^\dagger + h.c.) - \mu\sum_{j=1}^{N}(c_j^\dagger c_j - \frac{1}{2}), \tag{A6}$$

because we need them later on. In this case, $A-B$ and $A+B$ read,

$$A-B=\frac{1}{2}\begin{pmatrix} -2\mu & t_1-\Delta_1 & t_2-\Delta_2 & & & & & \\ t_1^*+\Delta_1 & -2\mu & t_1-\Delta_1 & t_2-\Delta_2 & & & \mathbf{0} & \\ t_2^*+\Delta_2 & t_1^*+\Delta_1 & -2\mu & t_1-\Delta_1 & t_2-\Delta_2 & & & \\ & & & \ddots & & & & \\ & & & t_2^*+\Delta_2 & t_1^*+\Delta_1 & -2\mu & t_1-\Delta_1 & t_2-\Delta_2 \\ & \mathbf{0} & & & t_2^*+\Delta_2 & t_1^*+\Delta_1 & -2\mu & t_1-\Delta_1 \\ & & & & & t_2^*+\Delta_2 & t_1^*+\Delta_1 & -2\mu \end{pmatrix}, \tag{A7}$$

$$A+B=\frac{1}{2}\begin{pmatrix} -2\mu & t_1+\Delta_1 & t_2+\Delta_2 & & & & & \\ t_1^*-\Delta_1 & -2\mu & t_1+\Delta_1 & t_2+\Delta_2 & & & \mathbf{0} & \\ t_2^*-\Delta_2 & t_1^*-\Delta_1 & -2\mu & t_1+\Delta_1 & t_2+\Delta_2 & & & \\ & & & \ddots & & & & \\ & & & t_2^*-\Delta_2 & t_1^*-\Delta_1 & -2\mu & t_1+\Delta_1 & t_2+\Delta_2 \\ & \mathbf{0} & & & t_2^*-\Delta_2 & t_1^*-\Delta_1 & -2\mu & t_1+\Delta_1 \\ & & & & & t_2^*-\Delta_2 & t_1^*-\Delta_1 & -2\mu \end{pmatrix}. \tag{A8}$$

For the Hamiltonian Eq. (A1), i.e. with $t_1=1$, $\Delta_1=\Delta$, and $t_2=\Delta_2=0$, these reduce to,

$$A-B=\frac{1}{2}\begin{pmatrix} -2\mu & 1-\Delta & & & & & & \\ 1+\Delta & -2\mu & 1-\Delta & & & & \mathbf{0} & \\ 0 & 1+\Delta & -2\mu & 1-\Delta & & & & \\ & & & \ddots & & & & \\ & & & & 1+\Delta & -2\mu & 1-\Delta & 0 \\ & \mathbf{0} & & & & 1+\Delta & -2\mu & 1-\Delta \\ & & & & & & 1+\Delta & -2\mu \end{pmatrix}, \tag{A9}$$

$$A+B=\frac{1}{2}\begin{pmatrix} -2\mu & 1+\Delta & & & & & & \\ 1-\Delta & -2\mu & 1+\Delta & & & & \mathbf{0} & \\ 0 & 1-\Delta & -2\mu & 1+\Delta & & & & \\ & & & \ddots & & & & \\ & & & & 1-\Delta & -2\mu & 1+\Delta & 0 \\ & \mathbf{0} & & & & 1-\Delta & -2\mu & 1+\Delta \\ & & & & & & 1-\Delta & -2\mu \end{pmatrix}. \tag{A10}$$

Using these matrices in Eq. (10) one gets

$$(1-\Delta^2)\phi_{\alpha,n-2}-4\mu\phi_{\alpha,n-1}+[4\mu^2+2(1+\Delta^2)]\phi_{\alpha,n}-4\mu\phi_{\alpha,n+1}+(1-\Delta^2)\phi_{\alpha,n+2}=4\Lambda_\alpha^2\phi_{\alpha,n}, \tag{A11}$$

for $3\leq n\leq N-2$. We call this the 'bulk equation'. In the case of periodic boundary conditions, this is actually the only equation one has to consider. However, for an open chain with free boundary conditions, we also have four boundary equations which are different from the bulk one, namely for $n=1,2,N-1$ and N one has:

$$[4\mu^2+(1-\Delta)^2]\phi_{\alpha,1}-4\mu\phi_{\alpha,2}+(1-\Delta^2)\phi_{\alpha,3}=4\Lambda_\alpha^2\phi_{\alpha,1} \qquad (n=1) \tag{A12}$$

$$-4\mu\phi_{\alpha,1}+[4\mu^2+2(1+\Delta^2)]\phi_{\alpha,2}-4\mu\phi_{\alpha,3}+(1-\Delta^2)\phi_{\alpha,4}=4\Lambda_\alpha^2\phi_{\alpha,2} \qquad (n=2) \tag{A13}$$

$$(1-\Delta^2)\phi_{\alpha,N-3}-4\mu\phi_{\alpha,N-2}+[4\mu^2+2(1+\Delta^2)]\phi_{\alpha,N-1}-4\mu\phi_{\alpha,N}=4\Lambda_\alpha^2\phi_{\alpha,N-1} \qquad (n=N-1) \tag{A14}$$

$$(1-\Delta^2)\phi_{\alpha,N-2}-4\mu\phi_{\alpha,N-1}+[4\mu^2+(1+\Delta)^2]\phi_{\alpha,N}=4\Lambda_\alpha^2\phi_{\alpha,N} \qquad (n=N). \tag{A15}$$

We note the difference between the $\phi_{\alpha,1}$ term in the equation for $n=1$ and the $\phi_{\alpha,N}$ term in the equation for $n=N$.

To solve these equations we can start with an ansatz for the eigenvalues Λ_α. Note that the bulk equation is the same for both the periodic and the open chain. This suggests to use our knowledge about the periodic case. The bulk equation determines the form of the eigenvalues as a function of a parameter α, which in turn is determined by the boundary equations. This is exactly what happens in the periodic case, where we use k instead of

α and fix $k = \dfrac{2\pi n}{N}$ for $n = 0, 1, \ldots N-1$ in Eq. (A4) by demanding $c_{N+1} = c_1$.

Therefore we use the same parametrization for the eigenvalues as in the open case,

$$\Lambda_\alpha^2 = (\mu - \cos\alpha)^2 + \Delta^2 \sin^2\alpha. \tag{A16}$$

Now we need to find an equation based on which one can determine all the possible values of α. With the ansatz for Λ_α, we solve Eq. (A11) by the standard approach, i.e. we consider $\phi_{\alpha,n} \sim x_\alpha^n$. Using this in Eq. (A11) gives us:

$$x_\alpha^4 - K x_\alpha^3 + 2(K\cos\alpha - \cos 2\alpha) x_\alpha^2 - K x_\alpha + 1 = 0, \tag{A17}$$

$$K = \frac{4\mu}{1-\Delta^2}. \tag{A18}$$

One checks that $e^{\pm i\alpha}$ are solutions independent of the parameter K. Since we have found two roots, we can find the other two, which are given by $e^{\pm i\beta}$ where β satisfies

$$\cos\alpha + \cos\beta = \frac{K}{2}. \tag{A19}$$

Therefore each α has a β partner. We note that α and β are equivalent. The associated eigenvalues can be written in the same functional form, i.e. $\Lambda_\alpha = \Lambda_\beta = \sqrt{(\mu - \cos\beta)^2 + \Delta^2 \sin^2\beta}$, which follows from Eq. (A19). We continue to use α as the label indicating the eigenvalue.

These solutions tell that $e^{\pm in\alpha}$ and $e^{\pm in\beta}$ are the most general solution for the bulk equation. Now we need to determine a linear combination of these functions that satisfies the boundary equations. Treating the left and right edges in an equivalent way, we consider the following combination:

$$\begin{aligned}\phi_{\alpha,n} = {} & A_1 \sin(n\alpha) + A_2 \sin[(N+1-n)\alpha] \\ & + B_1 \sin(n\beta) + B_2 \sin[(N+1-n)\beta]\ ,\end{aligned} \tag{A20}$$

in which A_1,A_2,B_1 and B_2 are constants.

Using this ansatz, Eqs. (A13) and (A14) give us:

$$A_1 \sin[(N+1)\alpha] + B_1 \sin[(N+1)\beta] = 0 \tag{A21}$$

$$A_2 \sin[(N+1)\alpha] + B_2 \sin[(N+1)\beta] = 0\ . \tag{A22}$$

Based on these relations, we rewrite the ansatz:

$$\begin{aligned}\phi_{\alpha,n} = {} & A_1 \Big\{ \sin(n\alpha) - \frac{\sin[(N+1)\alpha]}{\sin[(N+1)\beta]} \sin(n\beta) \Big\} \\ & + A_2 \Big\{ \sin[(N+1-n)\alpha] \\ & - \frac{\sin[(N+1)\alpha]}{\sin[(N+1)\beta]} \sin[(N+1-n)\beta] \Big\}.\end{aligned} \tag{A23}$$

Finally, we make sure that the ansatz satisfies Eqs. (A12) and (A15), which leads to the following equations:

$$\begin{pmatrix} -\dfrac{\Delta}{1-\Delta} f_3(\alpha,\beta) & -\dfrac{\Delta}{1-\Delta} f_1(\alpha,\beta) + f_2(\alpha,\beta) \\ \dfrac{\Delta}{1+\Delta} f_1(\alpha,\beta) + f_2(\alpha,\beta) & \dfrac{\Delta}{1+\Delta} f_3(\alpha,\beta) \end{pmatrix} \begin{pmatrix} A_1 \\ A_2 \end{pmatrix} = \begin{pmatrix} 0 \\ 0 \end{pmatrix} \tag{A24}$$

in terms of the functions

$$f_1(\alpha,\beta) = \sin(N\alpha) - \frac{\sin[(N+1)\alpha]}{\sin[(N+1)\beta]} \sin(N\beta) \tag{A25}$$

$$f_2(\alpha,\beta) = \sin[(N+1)\alpha](\cos\beta - \cos\alpha) \tag{A26}$$

$$f_3(\alpha,\beta) = \sin\alpha - \frac{\sin[(N+1)\alpha]}{\sin[(N+1)\beta]} \sin\beta\ . \tag{A27}$$

To find a non-trivial solution for A_1 and A_2, we require that the the determinant of the matrix in Eq. (A24) is zero. This gives us another equation for α and β:

$$\begin{aligned}& \sin^2\alpha + \sin^2\beta + \frac{1}{\Delta^2}(\cos\beta - \cos\alpha)^2 \\ & - 2\frac{\sin\alpha \sin\beta}{\sin[(N+1)\alpha]\sin[(N+1)\beta]} \\ & \times \Big\{ 1 - \cos[(N+1)\alpha]\cos[(N+1)\beta] \Big\} = 0.\end{aligned} \tag{A28}$$

This equation should be solved together with Eq. (A19) to give us all admissible labels. Generically, this has to be done numerically.

In the analysis below, we focus on the regime with $\mu \geq 0$ and $\Delta \geq 0$. We assume that $\Delta \neq 1$, the case $\Delta = t = 1$ was considered explicitly in[20,21]. From the equations (A28) and (A19), we see that a solution (α, β) for $\Delta > 0$ also gives a solution for $\Delta < 0$ (though the form of the wave function $\phi_{\alpha,n}$ changes). In addition,

the solutions for $\mu < 0$ can be related to the solutions with $\mu > 0$. If a pair (α, β) satisfies the equations for $\mu > 0$, the pair $(\alpha + \pi, \beta + \pi)$ will satisfy the equations for $\mu < 0$. Note that this shift does not change Eq. (A28). However, it gives rise to a minus sign in the left hand side of Eq. (A19) which indeed changes the sign of μ. Finally, the actual eigenvalues Λ_α are also unchanged.

Thus from now on, we assume that $\mu, \Delta \geq 0$. The structure of the solutions (α, β) is as follows. For $\mu > 1$, one finds N solutions, for which α and or β is real. Because α and β are completely equivalent, we assume that α is real. When $0 \leq \mu < 1$, there are $N-1$ solutions, with α real, and β either real or complex. We note that if β is complex, its real part $\mathrm{Re}\beta = 0$ for $\Delta < 1$, and $\mathrm{Re}\beta = \pi$ for $\Delta > 1$. The 'missing' solution has both α and β complex, and corresponds to the zero mode, which we describe in detail below. In Fig. 2, we show this for a chain of $N = 6$ sites, $\Delta = 0.8$ and different values of μ.

Before we do so, we first discuss the solutions with α real. We first note that for any (α, β) pair that solves Eqn. (A28) and (A19), all the combinations of $(\pm\alpha, \pm\beta)$ are also a solution. Since these pairs give rise to same wavefunction, we only consider α in the range $0 \leq \alpha \leq \pi$.

The solutions are then obtained by finding the solutions of Eq. (A28), where β is given by Eq. (A19). Special care has to be taken in the case that both α and β are real, say $(\alpha, \beta) = (\alpha_1, \beta_1)$, because one will also find the equivalent solution $(\alpha, \beta) = (\beta_1, \alpha_1)$, so one has to restrict the range of α further, to avoid 'double counting' of solutions.

From Eq. (A19) it is clear that α and β can only be both real when $-1 \leq \frac{\mu}{1-\Delta^2} \leq 1$. Because $\mu, \Delta \geq 0$, this leads to two regimes, $\Delta < \sqrt{1-\mu}$ and $\Delta > \sqrt{1+\mu}$. In these regimes, one always finds the solution $\alpha = \beta = \arccos(\mu/(1-\Delta^2)) = \alpha_c$, because Eq. (A28) is trivial when $\alpha = \beta$. This solution is not valid, however, because it leads to $\phi_{\alpha,n} = 0$.

Nevertheless, the value α_c is useful when specifying the appropriate range for α. If there are solutions with both α and β real, one has that either $\alpha < \alpha_c < \beta$, or $\beta < \alpha_c < \alpha$. In addition, for the range $\Delta \leq \sqrt{1-\mu}$, one finds that all the solutions (α, β) with β imaginary have $\alpha > \alpha_c$. Thus, to find all solutions in this range, one should only take the solutions for α such that $\alpha_c < \alpha < \pi$. For the range $\Delta \geq \sqrt{1+\mu}$, the situation is opposite, and one should take the solutions for α in the range $0 \leq \alpha < \alpha_c$. In the other regime, namely $\sqrt{1-\mu} < \Delta < \sqrt{1+\mu}$, one has to consider all solutions for α in the range $0 \leq \alpha < \pi$.

We now turn our attention to the Majorana zero mode solution. The goal is to find the analytical expression for the wave function of this mode. For simplicity, we work in the limit of large system size, i.e., $N \to \infty$.

By analyzing Eq. (A28), one finds that the solution one loses, is the one with smallest positive, real α. Taking the limit $\alpha \to 0$ and $N \to \infty$ of Eq. (A28), using Eq.(A19), gives

$$\frac{4}{\Delta^2(1-\Delta^2)}(\mu - 1)[\mu - (1-\Delta^2)] = 0 \qquad \text{(A29)}$$

This shows that there is a solution with $\alpha = 0$, for $\mu = 1$. In addition, further analysis shows that for $\mu < 1$, one losses this solution, both for $\Delta < 1$ and $\Delta > 1$, while for $\mu > 1$, this solution shifts to finite, positive α. This behavior can be seen for a chain with $N = 6$ sites, $\Delta = 0.8$ and $\mu = 1.2, 0.6, 0.25$ in Fig. 2. In the case of $\mu = 0.25$, only the solutions with $\alpha > \alpha_c \approx 0.25\pi$ are independent, so the there are still only five solutions. The additional, sixth solution is still a zero-mode.

We note that for finite N, the value of μ for which one loses the solution has $1/N$ corrections, and depends on Δ. That the phase transition between the trivial and topological phase occurs for $\mu = 1$ in the large N limit is of course well known, and is given by the value of μ for which the gap closes. Based on Eq. (A4), we infer that $\mu = \pm 1$ are the only possible values of chemical potential for which gap closes (provided that $\Delta \neq 0$).

Now we turn to finding the missing root and its associated features. To do so we need to consider different cases.

1) $\Delta < 1$ and $\sqrt{1-\Delta^2} < \mu < 1$: In this regime, we lost one solution with α real, so we look for a solution with both α and β imaginary, and in fact, purely real. Such a solution indeed exist namely,

$$\alpha^* = i(\frac{1}{\xi_1} - \frac{1}{\xi_2}), \qquad \beta^* = i(\frac{1}{\xi_1} + \frac{1}{\xi_2}), \qquad \text{(A30)}$$

$$\cosh\frac{1}{\xi_1} = \frac{1}{\sqrt{1-\Delta^2}}, \quad \cosh\frac{1}{\xi_2} = \frac{\mu}{\sqrt{1-\Delta^2}}, \qquad \text{(A31)}$$

which solves Eq. (A19) and Eq. (A28) in the large N limit. For $\sqrt{1-\Delta^2} < \mu < 1$, both ξ_1 and ξ_2 are real. Let us explore the properties of this solution. First, putting this result back into the Eq. (A16) gives us $\Lambda_{\alpha^*} = 0$, so we indeed have a zero-mode. This means that we can use Eq. (8) to solve for the wave function. Alternatively, we can set $A_1 = 0$ is Eq. (A23) to obtain the Majorana mode that is localized on the left side of the system. Either approach gives

$$\phi_{\alpha^*,n} = Ce^{-\frac{n}{\xi_1}}\sinh(\frac{n}{\xi_2}), \qquad \text{(A32)}$$

where C is a normalization constant. Because $\xi_1 < \xi_2$, the mode ϕ_{α^*} is indeed localized on the left edge.

The same reasoning can be done for $\psi_{\alpha,n}$. The important observation is that $(A+B)(A-B)$ has the same structure as $(A-B)(A+B)$ if we look at it from the other side of the chain. i.e. $n \to N+1-n$. So we get $\psi_{\alpha^*,n} = \phi_{\alpha^*,N+1-n}$, which tells us that $\psi_{\alpha^*,n}$ is localized on the right edge.

2) $\Delta < 1$ and $\mu < \sqrt{1-\Delta^2}$: For $\mu < \sqrt{1-\Delta^2}$, the parameter ξ_2 in Eq. (A30) becomes imaginary, so is more natural to rewrite the previous solution. Thus, the root can be written as:

$$\alpha^* = -q + i\frac{1}{\xi}, \qquad \beta^* = q + i\frac{1}{\xi}, \qquad \text{(A33)}$$

$$\cos q = \frac{\mu}{\sqrt{1-\Delta^2}}, \quad \cosh\frac{1}{\xi} = \frac{1}{\sqrt{1-\Delta^2}}. \qquad \text{(A34)}$$

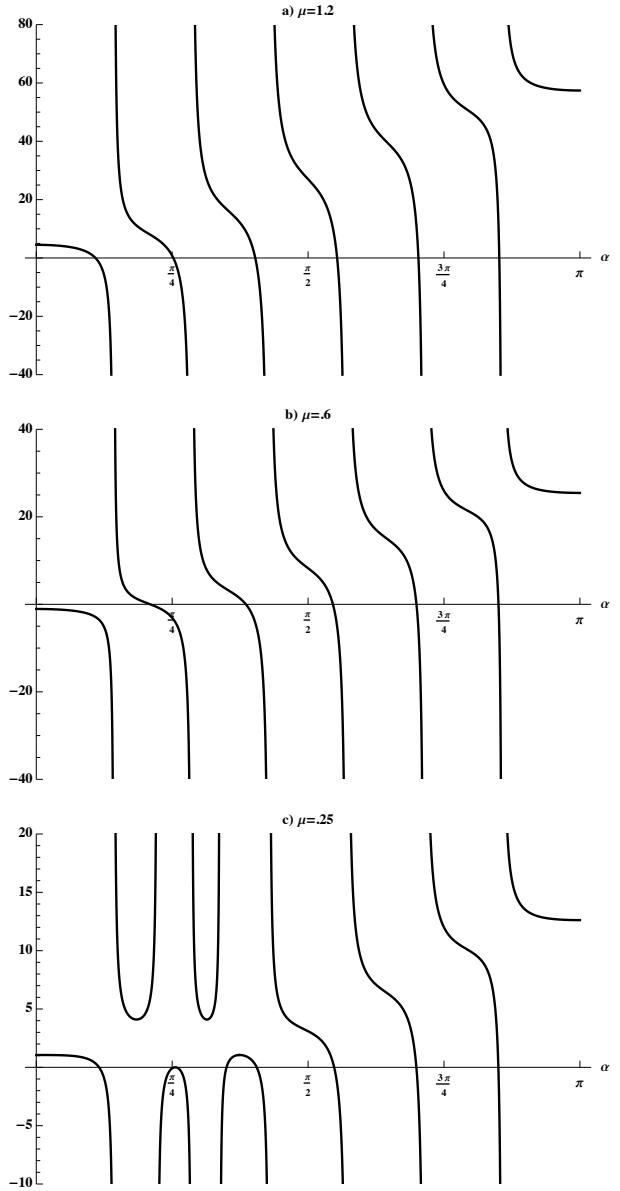

FIG. 2: Plot of the left hand side of the constraint Eq. (A28) as a function of α for $N = 6$, $\Delta = 0.8$ and $\mu = 1.2, 0.6, 0.25$ for a), b) and c) respectively. For $\mu = 1.2$, there are six solutions, so there are no zero-modes. For $\mu = .6$, there are five solutions. For $\mu = .25$, there are five independent solutions, which one can pick to lie in the range $\alpha > \alpha_c \approx 0.25\pi$.

Again, one finds that $\Lambda_{\alpha^*} = 0$. Using the same logic as above, one finds that

$$\phi_{\alpha^*,n} = Ce^{-\frac{n}{\xi}} \sin(nq), \tag{A35}$$

with C some constant. This result shows that ϕ_{α^*} is localized on the left edge. Although this in this case instead of having decaying functions, we have an oscillatory decaying function.

3) $\Delta > 1$: In this case we can not use the previous results, because $\sqrt{1-\Delta^2}$ becomes imaginary. One finds that the new root in this regime is given by

$$\alpha^* = i(\frac{1}{\xi_1} - \frac{1}{\xi_2}), \qquad \beta^* = \pi + i(\frac{1}{\xi_1} + \frac{1}{\xi_2}), \tag{A36}$$

$$\sinh\frac{1}{\xi_1} = \frac{1}{\sqrt{\Delta^2-1}}, \quad \sinh\frac{1}{\xi_2} = \frac{\mu}{\sqrt{\Delta^2-1}}. \tag{A37}$$

We see that $\xi_1 < \xi_2$ since $\mu < 1$. One can check that for this root $\Lambda_{\alpha^*} = 0$, hence it is also a zero mode. To find the Majorana mode that is localized on the left edge, we again set $A_1 = 0$ in Eq. (A23), which results in

$$\phi_{\alpha^*,n} = Ce^{-\frac{n}{\xi_1}} \times \begin{cases} \cosh(\frac{n}{\xi_2}), & \text{if } n \text{ is odd,} \\ \sinh(\frac{n}{\xi_2}) & \text{if } n \text{ is even.} \end{cases} \tag{A38}$$

This result shows that ϕ_{α^*} is localized on the left edge.

To close this section we note that for $\mu = \sqrt{1-\Delta^2}$, we have $\alpha^* = \beta^*$. Therefore one can not use x_α^n and x_β^n as separate solutions, but one should use nx_α^n as the other independent solution.

Appendix B: The zero-modes of the Kitaev chain with a phase gradient

In this appendix, we investigate the zero mode of the Kitaev chain, in the presence of a phase gradient in the order parameter. We assume that $|t| = |\Delta| = 1$.

As we mentioned in Sec. IV B, after a gauge transformation the Hamiltonian takes the form

$$H = \frac{1}{2}\sum_{j=1}^{N-1}(e^{i\frac{\nabla\theta}{2}}c_j^\dagger c_{j+1} + e^{-i\frac{\nabla\theta}{2}}c_j^\dagger c_{j+1}^\dagger + h.c) - \mu\sum_{j=1}^{N}(c_j^\dagger c_j - \frac{1}{2}), \tag{B1}$$

in which $\nabla\theta$ is the phase gradient per site, which is constant. To find the zero-mode, we use the method which is presented in Sec. II. From Eq. (A7) matrices $A - B$ and $A + B$ read

$$A-B=\begin{pmatrix} -\mu & i\sin(\frac{\nabla\theta}{2}) & & & & & \\ e^{-i\frac{\nabla\theta}{2}} & -\mu & i\sin(\frac{\nabla\theta}{2}) & & & \mathbf{0} & \\ 0 & e^{-i\frac{\nabla\theta}{2}} & -\mu & i\sin(\frac{\nabla\theta}{2}) & & & \\ & & & \ddots & & & \\ & & & & e^{-i\frac{\nabla\theta}{2}} & -\mu & i\sin(\frac{\nabla\theta}{2}) & 0 \\ & \mathbf{0} & & & & e^{-i\frac{\nabla\theta}{2}} & -\mu & i\sin(\nabla\theta\frac{\nabla\theta}{2}) \\ & & & & & & e^{-i\frac{\nabla\theta}{2}} & -\mu \end{pmatrix}, \tag{B2}$$

$$A+B=\begin{pmatrix} -\mu & \cos(\frac{\nabla\theta}{2}) & & & & \\ 0 & -\mu & \cos(\frac{\nabla\theta}{2}) & & \mathbf{0} & \\ & & \ddots & & & \\ & & & -\mu & \cos(\frac{\nabla\theta}{2}) & 0 \\ & \mathbf{0} & & & -\mu & \cos(\frac{\nabla\theta}{2}) \\ & & & & & -\mu \end{pmatrix}. \tag{B3}$$

In this case we are only looking for the zero mode and the corresponding Majorana operator. Hence we drop the α^* index. In order to have a Hermitian operator, ψ needs to be imaginary in Eq. (16). So we set $\psi = i\tilde{\psi}$ and $g_n = \frac{1}{2}(\phi_n + i\tilde{\psi}_n)$. First we look at the 'bulk equation' that follows from Eq. (15):

$$-\mu\tilde{\psi_n} + \cos(\frac{\nabla\theta}{2})\tilde{\psi}_{n-1} = 0. \tag{B4}$$

The only equation which is different from this bulk equation has index one (note that matrices are acting from the right on the vectors),

$$-\mu\tilde{\psi}_1 = 0. \tag{B5}$$

These two equations give us the solution:

$$\tilde{\psi}_n = R\Big[\frac{\mu}{\cos(\frac{\nabla\theta}{2})}\Big]^{N-n+1}, \tag{B6}$$

where R is a normalization constant. We see that the boundary equation holds (in the large N limit), provided that $\mu < \cos(\frac{\nabla\theta}{2})$, which precisely corresponds with the criterion to be in the topological phase, as we discussed in Sec. IV B.

We move on to find ϕ. The 'bulk equation' coming from Eq. (14) reads

$$-\mu\phi_n + \cos(\frac{\nabla\theta}{2})\phi_{n+1} = \sin(\frac{\nabla\theta}{2})(\tilde{\psi}_{n-1} - \tilde{\psi}_{n+1}). \tag{B7}$$

Here we encounter the first difference in comparison with the case with only real couplings. In this case the equation governing ϕ depends on $\tilde{\psi}$. This means that the general solution for ϕ consists of a part that satisfies Eq. (B7) with the right hand side set to zero, and a particular solution. The general solution takes the following form

$$\phi_n = L\Big[\frac{\mu}{\cos(\frac{\nabla\theta}{2})}\Big]^n - R\tan(\frac{\nabla\theta}{2})\Big[\frac{\mu}{\cos(\frac{\nabla\theta}{2})}\Big]^{N-n+1}, \tag{B8}$$

where the first term satisfies Eq. (B7) with the right hand side set to zero and the second term satisfies the full Eq. (B7). Thus, in this (unnormalized) solution, L is a free parameter. We note that the first term is localized on the left hand side of the system, while the second term is localized on the right hand side. We should also check the two boundary equations, which are given by:

$$n=1: \quad -\mu\phi_1 + \cos(\frac{\nabla\theta}{2})\phi_2 = -\sin(\frac{\nabla\theta}{2})\tilde{\psi}_2, \tag{B9}$$

$$n=N: \quad -\mu\phi_N = \sin(\frac{\nabla\theta}{2})\tilde{\psi}_{N-1}. \tag{B10}$$

By substituting the solution for ϕ and ψ back into Eqs.(B9) and (B10), we find that they are satisfied up to terms that are exponentially small in the large N limit.

Using this general solution, we can construct two solutions for g_n, that are localized on either side of the system. Setting $R = 0$, one finds a real solution (localized on the left) $g_n = L\Big[\frac{\mu}{\cos(\frac{\nabla\theta}{2})}\Big]^n$. Using Eq .(16), we see that the corresponding electron operator η_α operator only involves the operators $\gamma_{A,i}$, not the $\gamma_{B,i}$. The other solution, localized on the right, is found for $L = 0$, and is given by $g_n = \frac{R}{\cos(\frac{\nabla\theta}{2})} ie^{i\frac{\nabla\theta}{2}}\Big[\frac{\mu}{\cos(\frac{\nabla\theta}{2})}\Big]^{N-n+1}$. Thus, this right mode involves both $\gamma_{A,i}$ and $\gamma_{B,i}$. We note that the above solutions are valid in the limit of semi-infinite chains. In the case of a finite, but long chain, they can be combined to form an approximate solution (up to corrections that are exponentially small the length of the system) of the fermionic zero-mode, that is delocalized, with support on both ends of the chain.

[1] K. von Klitzing, G. Dorda, M. Pepper, Phys. Rev. Lett. **45**, 494 (1980).
[2] D.C. Tsui, H.L. Stormer, A.C. Gossard, Phys. Rev. Lett. **48**, 1559 (1982).
[3] X.-G.Wen, Adv. Phys., **44**, 405 (1995).
[4] A.Y. Kitaev, Phys. Usp. **44**, 131 (2001).
[5] Y. Oreg, G. Refael, F. von Oppen, Phys. Rev. Lett. **105**, 177002 (2010).
[6] R.M. Lutchyn, J.D. Sau, S. Das Sarma, Phys. Rev. Lett. **105**, 077001 (2010).
[7] V. Mourik, K. Zuo, S.M. Frolov, S.R. Plissard, E.P.A.M. Bakkers, L.P. Kouwenhoven, Science **336**, 1003 (2012).
[8] M.T. Deng, C.L. Yu, G.Y. Huang, M. Larsson, P. Caroff, H.Q. Xu, Nano Lett. **12**, 6414 (2012).
[9] A. Das, Y. Ronen, Y. Most, Y. Oreg, M. Heiblum, H. Shtrikman, Nat. Phys. **8**, 887 (2012).
[10] T.-P. Choy, J.M. Edge, A.R. Akhmerov, C.W.J. Beenakker, Phys. Rev. B **84**, 195442 (2011).
[11] F. Pientka, L.I. Glazman, F. von Oppen, Phys. Rev. B **88**, 155420 (2013).
[12] S. Nadj-Perge, I.K. Drozdov, B.A. Bernevig, A. Yazdani, Phys. Rev. B **88**, 020407(R) (2013).
[13] S. Nadj-Perge, I.K. Drozdov, J. Li, H. Chen, S. Jeon, A.H. MacDonald, B.A. Bernevig, A. Yazdani, Science **346**, 602 (2014).
[14] A.Y. Kitaev, Ann. Phys. **303**, 2 (2003).
[15] J. Alicea, Rep. Prog. Phys. **75**, 076501 (2012).
[16] J. Alicea, Y. Oreg, G. Refael, F. von Oppen, M.P.A. Fisher, Nat. Phys. **7**, 412 (2010).
[17] D. Aasen, M. Hell, R.V. Mishmash, A. Higginbotham, J. Danon, M. Leijnse, T.S. Jespersen, J.A. Folk, C.M. Marcus, K. Flensberg, J. Alicea, Phys. Rev. X **6**, 031016 (2016).
[18] D. Sticlet, C. Bena, P. Simon, Phys. Rev. B **87**, 104509 (2013).
[19] E. Lieb, T. Schultz, D. Mattis, Ann. Phys. **16**, 407 (1961).
[20] R.J. Elliott, P. Pfeuty, C. Wood, Phys. Rev. Lett. **25**, 443 (1970);
[21] P. Pfeuty, Ann. Phys. **57**, 79 (1970).
[22] S.S. Hegde, S. Vishveshwara, Phys. Rev. B **94**, 115166 (2016).
[23] E. Barouch, B.M. McCoy, Phys. Rev. A 3, 786 (1971).
[24] M. Suzuki, Prog. Theor. Phys. **71**, 1337 (1971).
[25] M. Henkel, *Conformal invariance and critical phenomena*, Springer, Berlin (1999).
[26] Y. Niu, S.B. Chung, C-H. Hsu, I. Mandal, S. Raghu, S. Chakravarty, Phys. Rev. B **85**, 035110 (2012).
[27] A.C. Doherty, S.D. Bartlett, Phys. Rev. Lett. **103**, 020506 (2009).
[28] T. Ohta, S. Tanaka, I. Danshita, K. Totsuka, J. Phys. Soc. Jpn. **84**, 063001 (2015).
[29] V. Lahtinen, E. Ardonne, Phys. Rev. Lett. **115**, 237203 (2015).
[30] T. Ohta, S. Tanaka, I. Danshita, K. Totsuka, Phys. Rev. B **93**, 165423 (2016).
[31] A. Kitaev, AIP Conf. Proc. **1134**, 22 (2009).
[32] S. Ryu, A.P. Schnyder, A. Furusaki, A.W.W. Ludwig New J. Phys. **12**, 065010 (2010).
[33] L. Fidkowski, A. Kitaev, Phys. Rev. B **81**, 134509 (2010).
[34] A. Romito, J. Alicea, G. Refael, F. von Oppen, Phys. Rev. B **85**, 020502 (2012).
[35] S. Tewari, J.D. Sau, Phys. Rev. Lett. **109**, 150408 (2012).
[36] F.K. Kunst, M. Trescher, E.J. Bergholtz, Phys. Rev. B **96**, 085443 (2017).

Exact ground states and edge modes of a $\mathbb{Z}_3$ quantum clock model and spin-S chains DRAFT!

Iman Mahyaeh and Eddy Ardonne
Department of Physics, Stockholm University, SE-106 91 Stockholm, Sweden
(Dated: December 11, 2017)

In this paper, we generalize the Peschel-Emery line of the interacting transverse field Ising model to a model based on three-state clock variables. Along a founded line, the model has exactly degenerate ground states, which can be written as product form. In addition, we present operators that transform these ground states into each other. Such operators are also presented for the Peschel-Emery case. Furthermore, we study the spin-S generalization of interacting Ising model and show that along Peschel-Emery line they also have degenerate ground states which is a product state. We also discuss some examples of excited states of all of these models, that can be obtained exactly in an analytic form.

PACS numbers:

Kitaev's work on Majorana bound states (MBS) [1] spurred the current interest in zero modes in general. This resulted in proposals to detect MBSs in nanowires [2, 3], resulting in several promising experiments [4–6], trying to observe these zero modes, which if observed, could be used for quantum information purposes.

From a theoretical point of view, one can divide zero modes in two types [7]. A zero mode is weak, if it is associated with a degeneracy only of the ground state, while a strong zero mode implies that the whole spectrum is degenerate (up to corrections that are exponentially small in the size of the system). Zero modes of non-interacting systems are strong, as for instance the MBSs of the non-interacting Kitaev chain. Other examples of interacting systems with a strong zero mode are the XYZ chain [8] and the *chiral* 3-state Potts model [9]. The zero-modes of the later model are interesting, because they are closely related to parafermionic zero-modes, which are more powerful in comparison to the MBS, and there are proposals to realize parafermions [7, 10, 11].

In this paper we are interested in interacting systems, that can be fine tuned such that they have an *exact* zero mode for arbitrary system size, i.e., models which have an exact degeneracy of the ground state. The excited states of these models are not degenerate.

Famous examples of models with an exact zero mode are the AKLT [12, 13] and Majumdar-Ghosh spin chains [14, 15], as well as the interacting transverse field Ising model, along the so-called Peschel-Emery (PE) line [16]. The common denominator of these models is that their ground states are frustration free. These ground states minimize the energy for each term in the Hamiltonian, even though these terms in the Hamiltonian do not commute with one another. Obviously, to achieve this, one has to fine tune the model. This is nevertheless a useful exercise, because for these fine tuned models, one can often prove much more results, such as the existence of gap, in comparison to generic Hamiltonians.

The main result of this paper is the generalization of the PE-line, to a model build from 3-state clock variables, such as the three state Potts model. Along this line, the three ground states are exactly degenerate, and can be written as product states. In addition, we construct edge operators, that permutes these ground states, all along this line. We also construct such an operator for the PE line, which was not known previously, and present some exact excited states of these models. Finally we introduce a spin-S generalization of the PE-line.

The Peschel-Emery line — The Hamiltonians we consider in this paper are all written as a sum of two-body terms of a L-site chain,

$$H = \sum_j h_{j,j+1} \ , \tag{1}$$

where the range of the sum changes depends on whether we consider an open or closed chain. For the Ising model in a magnetic field and pair interactions, Peschel and Emery [16] found that if one parametrizes $h_{j,j+1}(l)$ as follows,

$$h^{\mathrm{PE}}_{j,j+1}(l) = -\sigma^x_j\sigma^x_{j+1} + \frac{h(l)}{2}(\sigma^z_j + \sigma^z_{j+1}) + U(l)\sigma^z_j\sigma^z_{j+1} \tag{2}$$

the model has two exactly degenerate ground states, which can be written as product states. Here, the σ^α are the Pauli matrices and $U(l) = \frac{1}{2}[\cosh(l) - 1]$, $h(l) = \sinh(l)$ (we note that the sign of $h(l)$ is immaterial) and $l \geq 0$. The model is $\mathbb{Z}_2$ symmetric, with the parity given by $P = \prod_{j=1}^{L} \sigma^z_j$. In the open case, the magnetic field of the boundary spins is half that of the bulk spins.

A direct way to obtain $h^{\mathrm{PE}}_{j,j+1}$ was given by Katsura et al. [17]. For the two site problem, one first demands that the energy of the ground states in the even and odd sectors are equal, fixing the form of $h(l)$ and $U(l)$. Then one combines the two ground states to write them as product states. This ensures that the ground states of a chain of arbitrary length L are frustration free and can be written as product states. For both for the open and periodic chain, they take the form

$$|\psi^+(l)\rangle = (|\uparrow\rangle + \alpha|\downarrow\rangle)^{\otimes L}, |\psi^-(l)\rangle = (|\uparrow\rangle - \alpha|\downarrow\rangle)^{\otimes L} \ ,$$

where $\alpha = \exp(l/2)$ and the energy per bond is $\epsilon(l) = -(U(l)+1)$. These product states do not have definite parity, but parity states are constructed as

$$|P = \pm 1\rangle = |\psi^+(l)\rangle \pm |\psi^-(l)\rangle \ . \tag{3}$$

The fermionic incarnation of the model Eq. (2), obtained after performing a Jordan-Wigner transformation [18], is the Kitaev chain with a nearest-neighbor Hubbard term [17]. Along the PE-line, this model is in the topological phase [17, 19], and has exact zero modes in the open case. For $U = 0$ and arbitrary h the fermionic model is quadratic and can be solved [20–22]. For $|h| < 1$ the model is topological and hosts two Majorana zero edge modes [1]. The presence of this zero mode implies that the full spectrum is degenerate up to an exponentially small correction in the system size. Generically, upon adding the interaction term, one loses the degeneracy of the full spectrum [23] but as long one is in the topological phase, the ground state remains degenerate, so that the system has a *weak* zero mode, that resides on the edges of the system, and maps the ground states into each other.

We now construct edge operators along the full PE-line, but it is insightful to first consider $l = 0$. Using fermion language, such that we associated to Majorana operators $\gamma_{A,j}$ and $\gamma_{B,j}$ to each site j, the Majorana edge modes are completely localized on the first and last sites for $l = 0$. In the spin language one of these has a non-local string operator owing to the Jordan-Wigner transformation,

$$\gamma_{A,1} = \sigma_1^x \qquad\qquad \gamma_{B,L} = -iP\sigma_L^x. \tag{4}$$

These Majorana operators anti-commute with P and in the ground state space $\{|\psi^+(0)\rangle, |\psi^-(0)\rangle\}$, they act as σ^z and $-\sigma^y$ respectively.

We want to generalize these operators to arbitrary l such that they act on the ground state space in the same way and are normalized (i.e., square to the identity). The edge operators that satisfy these conditions are

$$A_{\frac{1}{2}}(l) = \frac{1}{\alpha}\sigma_1^+ + \alpha\sigma_1^-, \quad B_{\frac{1}{2}}(l) = -iP\left(\frac{1}{\alpha}\sigma_L^+ + \alpha\sigma_L^-\right), \tag{5}$$

where $\sigma^\pm = \frac{1}{2}(\sigma^x \pm i\sigma^y)$. They indeed act on the ground states as follows,

$$A_{\frac{1}{2}}(l)|\psi^+(l)\rangle = |\psi^+(l)\rangle,\ A_{\frac{1}{2}}(l)|\psi^-(l)\rangle = -|\psi^-(l)\rangle, \tag{6}$$

$$B_{\frac{1}{2}}(l)|\psi^+(l)\rangle = -i|\psi^-(l)\rangle,\ B_{\frac{1}{2}}(l)|\psi^-(l)\rangle = i|\psi^+(l)\rangle. \tag{7}$$

We note that despite the fact that $A_{\frac{1}{2}}(l)^2 = B_{\frac{1}{2}}(l)^2 = \mathbf{1}$ and $\{A_{\frac{1}{2}}(l), B_{\frac{1}{2}}(l)\} = 0$, these are not Majorana operators, because $A^\dagger_{\frac{1}{2}}(l) \neq A_{\frac{1}{2}}(l)$ and $B^\dagger_{\frac{1}{2}}(l) \neq B_{\frac{1}{2}}(l)$ for $l \neq 0$. Because $A^\dagger_{\frac{1}{2}}(l)$ and $B^\dagger_{\frac{1}{2}}(l)$ do not have a simple action on the ground state space, it does not seem possible to use them to construct Majorana operators with the desired action on the ground state space. Despite this, they do constitute an exact zero-mode, all along the PE-line.

The Majumdar-Ghosh [14, 15] and AKTL [12, 13] chains, which have frustration free ground states, also have excited states that can be obtained exactly for finite system size, see [24] and [25, 26] respectively. Along the PE-line, one can also obtain exact excited states, in the case with PBC and an even number of sites. We start with the eigenstates of $h_{j,j+1}(l)$

$$|g_+\rangle = |\uparrow\uparrow\rangle + e^l|\downarrow\downarrow\rangle \qquad |g_-\rangle = e^{l/2}(|\uparrow\downarrow\rangle + |\downarrow\uparrow\rangle) \tag{8}$$

$$|e_+\rangle = |\uparrow\uparrow\rangle - e^{-l}|\downarrow\downarrow\rangle \quad |e_-\rangle = (|\uparrow\downarrow\rangle - |\downarrow\uparrow\rangle) \tag{9}$$

where the ground states $g_\pm$ of both parity sectors have energy $\epsilon(l)$, while e_- and e_+ have energy $\epsilon(l)+2$ and $\epsilon(l)+2+U(l)$ respectively. For simplicity, we dropped the ket notation and the dependence on l. For a system with an even number of sites, i.e. $L = 2N$, the ground states can be written as

$$|P = \pm 1\rangle = \sum_{i_1\cdots i_N = \pm} g_{i_1} g_{i_2} \cdots g_{i_{N-1}} g_{i_N} \ , \tag{10}$$

where the sum is over all 2^{N-1} configurations $i_j = \pm$, with fixed overall parity. Both these parity ground states have momentum $K = 0$, despite the fact that the expression has a two-site block structure. Some exact excited states can be obtained by exchanging a ground state block g by an excited state block $e_\pm$, and summing over all positions for this block. Two parity states with $\Delta E = 4$ can be written as

$$|\Delta E = 4, \pm\rangle = \sum_{j=1}^{N} \sum_{i_1\cdots i_N = \pm} g_{i_1} \cdots g_{i_{j-1}} e_- g_{i_{j+1}} \cdots g_{i_N} \ , \tag{11}$$

where $i_j = -$ is fixed in the second sum. These states automatically have momentum $K = \pi$. Exchanging the block e_- by e_+ gives two excited states with energy $\Delta E = 4 + 4U(l)$. One starts with

$$|\Psi, \pm\rangle = \sum_{j=1}^{N} \sum_{i_1\cdots i_N = \pm} g_{i_1} \cdots g_{i_{j-1}} e_+ g_{i_{j+1}} \cdots g_{i_N} \ ,$$

and constructs $K = \pi$ states as follows

$$|\Delta E = 4 + 4U(l), \pm\rangle = |\Psi, \pm\rangle - T|\Psi, \pm\rangle \ , \tag{12}$$

where T translates the system by one site. Finally, by introducing both one e_- block and one e_+ block at positions j_1 and j_2, and summing over these positions, results in the states $|\Psi', \pm\rangle$. From these, one obtains two $K = 0$ states with energy $\Delta E = 8 + 4U(l)$,

$$|\Delta E = 8 + 4U(l), \pm\rangle = |\Psi', \pm\rangle + T|\Psi', \pm\rangle \ . \tag{13}$$

It is straightforward to convince oneself for small system sizes that the states presented here are indeed exact excited states. Proving this is less straightforward, despite the fact that one has the explicit form of both the Hamiltonian and the states.

The 3-state clock model — The construction of the PE-line can be generalized to the 3-state clock or Potts type models. The Hamiltonian of the 3-state clock model, which is a generalization of the transverse field Ising model is

$$H = -\sum_{j=1}^{L-1}(X_j^\dagger X_{j+1} + \text{h.c.}) - \sum_{j=1}^{L}(fZ_j^\dagger + \text{h.c.}) \ . \quad (14)$$

To each site, one associates a three-dimensional Hilbertspace, $|n\rangle$ with $n = 0, 1, 2$ taken modulo 3. The clock operators Z and X act as $Z|n\rangle = \omega^n|n\rangle$ with $\omega = \exp(i\frac{2\pi}{3})$ and $X|n\rangle = |n-1\rangle$. These operators satisfy $X^3 = Z^3 = \mathbf{1}$, $X^2 = X^\dagger$, $Z^2 = Z^\dagger$ and $XZ = \omega ZX$. Although this model is not solvable in general, it is known that for $|f| < 1$ this model has three degenerate ground states, while for $|f| > 1$ it shows a paramagnetic behavior (*ref?*).

The clock model Hamiltonian commutes with the parity operator which is now defined as $P = \prod_{j=1}^{L} Z$, hence Hamiltonian is $\mathbb{Z}_3$ symmetric. Therefore states can be labeled with their parity eigenvalue, $P = \omega^Q$, in which Q could be 0, 1 or 2 since $P^3 = \mathbf{1}$. Phase diagram of this model and it's chiral generalization [30] and the presence of parafermionic zero modes and their stability have been investigated [9, 27]. It was conjectured that in a finite region of phase space of couplings in the chiral model there is a *Strong* parafermionic edge zero mode which is normalizable and gives rise to three-fold degeneracy in the full many-body spectrum up to an exponentially small correction in the system size. A recent study, however, showed that the three-fold degeneracy of the full spectrum falls apart due to quantum resonances [31]

Apart from the integrable points of the model [32], the clock model has not been solved. Recently, Iemini et al [28] found a generalization in which the ground state is three-fold degenerate along a specific line and has a matrix-product form which becomes simple in terms of Fock parafermions [33]. Nevertheless, one can look for an extension of the model, and fine-tune the couplings, such that the ground states can be written as a product state, in analogy with the PE line.

We use the method [17] which has been outlined in the previous section. One first needs to establish which terms to add to the Hamiltonian Eq. (14). It turns out that one needs both the terms Z_jZ_{j+1} and $Z_jZ_{j+1}^\dagger$. With these terms, one finds putting the following two-site Hamiltonian in Eq.1 does the job,

$$h_{j,j+1}^{Z_3}(r) = -X_j^\dagger X_{j+1} - f(r)(Z_j + Z_{j+1}) - g_1(r)Z_jZ_{j+1} - g_2(r)Z_jZ_{j+1}^\dagger + \text{h.c.} \ . \quad (15)$$

The parameters are given by

$$f(r) = (1+2r)(1-r^3)/(9r^2) \quad (16)$$
$$g_1(r) = -2(1-r)^2(1+r+r^2)/(9r^2) \quad (17)$$
$$g_2(r) = (1-r)^2(1-2r-2r^2)/(9r^2) \ , \quad (18)$$

where $r > 0$ and $r = 1$ corresponds to the non-interacting model. Note that as for the PE-line, the 'magnetic field' term is half as strong on the boundary sites in comparison to the bulk sites. This model has three exactly degenerate ground states, with the energy per bond $\epsilon(r) = -2(1+r+r^2)^2/(9r^2)$. These ground states can, by construction, be written as product states,

$$|G_0(r)\rangle = (|0\rangle + r|1\rangle + r|2\rangle)^{\otimes L} \quad (19)$$
$$|G_1(r)\rangle = (|0\rangle + r\omega|1\rangle + r\bar{\omega}|2\rangle)^{\otimes L} \quad (20)$$
$$|G_2(r)\rangle = (|0\rangle + r\bar{\omega}|1\rangle + r\omega|2\rangle)^{\otimes L} \ . \quad (21)$$

These product states can be combined to form parity eigenstates,

$$|Q=0\rangle = |G_0(r)\rangle + |G_1(r)\rangle + |G_2(r)\rangle \quad (22)$$
$$|Q=1\rangle = |G_0(r)\rangle + \bar{\omega}|G_1(r)\rangle + \omega|G_2(r)\rangle \quad (23)$$
$$|Q=2\rangle = |G_0(r)\rangle + \omega|G_1(r)\rangle + \bar{\omega}|G_2(r)\rangle \ . \quad (24)$$

As was the case for the PE-line, one can explicitly construct edge operators for the open chain. For $r = 1$, the couplings f, g_1, g_2 are zero and we are left with $h_{j,j+1}^{Z_3}(1) = -X_jX_{j+1}^\dagger + \text{h.c.}$. In this limit one finds, using the Fradkin-Kadanoff transformation [29] to transform the clock degrees of freedom to parafermions $\eta_{A,j}$ and $\eta_{B,j}$, that the Hamiltonian does not depend on two of the parafermions [9], namely

$$\eta_{A,1} = X_1 \qquad \eta_{B,L} = \omega P X_L \ . \quad (25)$$

These operators obey the parafermion algebra, $\eta_{A,1}^3 = \eta_{B,L}^3 = \mathbf{1}$ and $\eta_{A,1}\eta_{B,L} = \omega\eta_{B,L}\eta_{A,1}$. To find edge modes for arbitrary r, we first note that $\eta_{A,1}$ and $\eta_{B,L}$ act on the ground state space $\{|G_0\rangle, |G_1\rangle, |G_2\rangle\}$ (with $r = 1$) as Z and $ZX^\dagger$. To generalize these operators to arbitrary r, it is useful to consider the generalization of the ladder operators for $SU(2)$ spins, namely

$$\Sigma^0 = \frac{X}{3}\left(\mathbf{1} + Z + Z^\dagger\right) \quad (26)$$
$$\Sigma^1 = \frac{X}{3}\left(\mathbf{1} + \bar{\omega}Z + \omega Z^\dagger\right) \quad (27)$$
$$\Sigma^2 = \frac{X}{3}\left(\mathbf{1} + \omega Z + \bar{\omega}Z^\dagger\right) \ . \quad (28)$$

One checks that $\Sigma^0|0\rangle = |2\rangle$, $\Sigma^1|1\rangle = |0\rangle$ and $\Sigma^2|2\rangle = |1\rangle$ while all the other matrix elements are zero.

The edge operators that act in the same way as $\eta_{A,1}$ and $\eta_{B,L}$ for arbitary r can be written in terms of the Σ^α's as

$$A_{Z_3}(r) = \frac{1}{r}\Sigma_1^1 + \Sigma_1^2 + r\Sigma_1^0, \quad (29)$$
$$B_{Z_3}(r) = \omega P\left(\frac{1}{r}\Sigma_L^1 + \Sigma_L^2 + r\Sigma_L^0\right) \ . \quad (30)$$

One can check that,

$$A_{Z_3}(r)|G_j\rangle = \omega^j|G_j\rangle \quad B_{Z_3}(r)|G_j\rangle = \omega^{j+1}|G_{j+1}\rangle \ , \quad (31)$$

where the index of $G_j(r)$ is taken modulo 3. So, indeed, A_{Z_3} acts as Z and B_{Z_3} as $ZX^\dagger$ in the space of ground states. Although these operators obey the relations $(A_{Z_3})^3 = (B_{Z_3})^3 = \mathbf{1}$ and $A_{Z_3}B_{Z_3} = \omega B_{Z_3}A_{Z_3}$, they are not parafermions, because for instance $A_{Z_3}^\dagger \neq (A_{Z_3})^2$, and similar for B_{Z_3}. This is exactly the same behavior as we found for the spin-1/2 PE-line. Again, the operators $A_{Z_3}(r)$ and $B_{Z_3}(r)$ are exact zero modes.

We now present three exact excited states for the model with PBC and $L = 2N$. Solving $h_{j,j+1}^{Z_3}$ gives us three ground states and two special excited states which are building blocks of our construction,

$$|g_1\rangle = |00\rangle + r^2|12\rangle + r^2|21\rangle, \tag{32}$$

$$|g_\omega\rangle = r^2|22\rangle + r|01\rangle + r|10\rangle, |e_\omega\rangle = |10\rangle - |01\rangle \tag{33}$$

$$|g_{\bar\omega}\rangle = r^2|11\rangle + r|02\rangle + r|20\rangle, |e_{\bar\omega}\rangle = |20\rangle - |02\rangle, \tag{34}$$

where $g_{1,\omega,\bar\omega}$ have energy $\epsilon(r)$, however, $e_{\omega,\bar\omega}$ have energy $\epsilon(r)+2+r$. We can rewrite three ground states in terms of these blocks,

$$|P = 1, \omega, \bar\omega\rangle = \sum_{i_1\cdots i_N = 1,\omega,\bar\omega} g_{i_1}g_{i_2}\cdots g_{i_{N-1}}g_{i_N} \ , \tag{35}$$

where the sum is over all 3^{N-1} configurations $i_j = 1, \omega, \bar\omega$, i.e. fixed parity. There three exact excited state with energy $\Delta E = 2(2+r)$ and momentum $K = \pi$ along the line which can be constructed by replacing one of 'g_i-blocks' by an 'e_i-block' with the same parity and performing the sum over all the blocks,

$$|\Delta E = 2(r+2), P = 1, \omega, \bar\omega\rangle = \sum_{j=1}^{N}(Z_{2j-1} - Z_{2j} + h.c.)|P = 1, \omega, \bar\omega\rangle \ . \tag{36}$$

Spin-S PE-line — We study the spin-S generalization of the PE-line which has been investigated previously [34–36]. Here we present the exact ground state wave functions, which again are product states, as well as the exact edge modes. The Hamiltonian for this model is

$$h_{j,j+1}^{\mathrm{S-PE}} = -S_j^x S_{j+1}^x + \frac{h(l)}{2}S\left(S_j^z + S_{j+1}^z\right) + U(l)S_j^z S_{j+1}^z, \tag{37}$$

in which S^α are spin operators of the the spin-S representation of $SU(2)$ algebra. The parameters $U(l) = \frac{1}{2}[\cosh(l) - 1]$ and $h(l) = \sinh(l)$, are the same as the PE-line couplings in Eq.2 [37]. The Hamiltonian Eq. (37) commutes with the 'parity' of the magnetization, $P_M = \prod_{j=1}^{L} e^{i\pi(S - S_j^z)}$, because the operators $S_j^x S_{j+1}^x$ either change the magnetization by two units, or leave it the same.

The model has two exactly degenerate ground states for arbitrary l, which can be written as product states, similar to the Z_2 and Z_3-clock model cases. These two ground states are

$$|\psi_S^+(l)\rangle = \left(e^{\alpha S^-}|S\rangle_z\right)^{\otimes L} \quad |\psi_S^-(l)\rangle = \left(e^{-\alpha S^-}|S\rangle_z\right)^{\otimes L} \ , \tag{38}$$

where $\alpha = \exp(\frac{l}{2})$ and $|S\rangle_z$ is the $S_z = S$ eigenstate, i.e. $S^z|S\rangle_z = S|S\rangle_z$. The states $|\psi_S^\pm(l)\rangle$ are not parity eigenstates, but these can be constructed as $|P_M = \pm\rangle = |\psi_S^+(l)\rangle \pm |\psi_S^-(l)\rangle$. As in the previous cases, these states are exact ground states for both the open and periodic chains, with the energy per bond given by $\epsilon_S(l) = -S^2(U(l)+1)$.

Following the $\mathbb{Z}_2$ case we define edge operators which act on the ground states,

$$A_S(l) = \frac{1}{2S}(\frac{1}{\alpha}S_1^+ + \alpha S_1^-) \tag{39}$$

$$B_S(l) = -\frac{i}{2S}P_M(\frac{1}{\alpha}S_L^+ + \alpha S_L^-) \ . \tag{40}$$

For $S = 1/2$, these operators reduce to $A_{\frac{1}{2}}(l)$ and $B_{\frac{1}{2}}(l)$ in Eq. (5). They act like σ^z and $-\sigma^y$ on the ground states, again in correspondence to the Z_2 case.

The model Eq. (37) with PBC has exact excited states, that are constructed from eigenstates of the two-site open model. The ground states $|g_\pm\rangle$ with parities $P_M = \pm 1$ are obtained by acting on $|S, S\rangle$ as

$$|g_\pm\rangle = \left[e^{\alpha(S_1^- + S_2^-)} \pm e^{-\alpha(S_1^- + S_2^-)}\right]|S, S\rangle \ . \tag{41}$$

There are two parity eigenstates $|e_\pm\rangle$ with energy $\Delta E = S$, which can be obtained from the ground states[38],

$$|e_\pm\rangle = (S_1^z - S_2^z)|g_\pm\rangle \ . \tag{42}$$

We first re-write the ground states of the $L = 2N$ site chain in terms of the $g_\pm$, in the same way as in the case of the PE-line, Eq. (10),

$$|P_M = \pm 1\rangle = \sum_{i_1\cdots i_N = \pm} g_{i_1}g_{i_2}\cdots g_{i_{N-1}}g_{i_N} \ , \tag{43}$$

where the sum is again over all 2^{N-1} configurations $i_j = \pm$, with fixed parity. These states are ground states of both the open and periodic chains, in the latter case they have momentum $K = 0$. From these $K = 0$ states, one obtains $K = \pi$, parity eigenstates with energy $\Delta E = 2S$, by replacing the one of 'g_i-blocks' by an 'e_i-block' with the same parity, and summing over the position,

$$|\Delta E = 2S, P_M = \pm 1\rangle = \sum_{j=1}^{N}(S_{2j-1}^z - S_{2j}^z)|P_M = \pm 1\rangle \ . \tag{44}$$

Acknowledgments — We would like to thank L. Mazza, C. Mora, N. Regnault and D. Schuricht for interesting discussions. This work was sponsored, in part, by the Swedish Research Council.

[1] A.Y. Kitaev, *Unpaired Majorana fermions in quantum wires*, Phys. Usp. **44**, 131 (2001), doi:10.1070/1063-7869/44/10S/S29.

[2] Y. Oreg, G. Refael, F. von Oppen, *Helical Liquids and Majorana Bound States in Quantum Wires*, Phys. Rev. Lett. **105**, 177002 (2010), doi:10.1103/PhysRevLett.105.177002.

[3] R.M. Lutchyn, J.D. Sau, S. Das Sarma, *Majorana Fermions and a Topological Phase Transition in Semiconductor-Superconductor Heterostructures*, Phys. Rev. Lett. **105**, 077001 (2010), doi:10.1103/PhysRevLett.105.077001.

[4] V. Mourik, K. Zuo, S.M. Frolov, S.R. Plissard, E.P.A.M. Bakkers, L.P. Kouwenhoven, *Signatures of Majorana Fermions in Hybrid Superconductor-Semiconductor Nanowire Devices*, Science **336**, 1003 (2012), doi:10.1126/science.1222360.

[5] M.T. Deng, C.L. Yu, G.Y. Huang, M. Larsson, P. Caroff, H.Q. Xu, *Anomalous Zero-Bias Conductance Peak in a NbInSb NanowireNb Hybrid Device*, Nano Lett. **12**, 6414 (2012), doi:10.1021/nl303758w.

[6] A. Das, Y. Ronen, Y. Most, Y. Oreg, M. Heiblum, H. Shtrikman, *Zero-bias peaks and splitting in an Al-InAs nanowire topological superconductor as a signature of Majorana fermions*, Nat. Phys. **8**, 887 (2012), doi:10.1038/nphys2479.

[7] J. Alicea, P. Fendley, *Topological Phases with Parafermions: Theory and Blueprints*, Annu. Rev. Cond. Mat. Phys. **7** 119 (2016), doi:10.1146/annurev-conmatphys-031115-011336.

[8] P. Fendley, *Strong zero modes and eigenstate phase transitions in the XYZ/interacting Majorana chain*, J. Phys. A: Math. Theor. **49**, 30LT01 (2016), doi:10.1088/1751-8113/49/30/30LT01.

[9] P. Fendley, *Parafermionic edge zero modes in Z_n-invariant spin chains*, J. Stat. Mech. P11020 (2012), doi:10.1088/1742-5468/2012/11/P11020.

[10] R.S.K. Mong, D.J. Clarke, J. Alicea, N.H. Lindner, P. Fendley, C. Nayak, Y. Oreg, A. Stern, E. Berg, K. Shtengel, M.P.A. Fisher, *Universal topological quantum computation from a superconductor/Abelian quantum Hall heterostructure*, Phys. Rev. X **4**, 011036 (2014), doi:10.1103/PhysRevX.4.011036.

[11] A. Vaezi, *Superconducting analogue of the parafermion fractional quantum Hall states*, Phys. Rev. X **4**, 031009 (2014), doi:10.1103/PhysRevX.4.031009.

[12] I. Affleck, T. Kennedy, E.H. Lieb, H. Tasaki, *Rigorous results on valence-bond ground states in antiferromagnets*, Phys. Rev. Lett. **59**, 799 (1987), doi:10.1103/PhysRevLett.59.799.

[13] I. Affleck, T. Kennedy, E.H. Lieb, H. Tasaki, *Valence bond ground states in isotropic quantum antiferromagnets*, Commun. Math. Phys. **115**, 477 (1988), doi:10.1007/BF01218021.

[14] C.K. Majumdar, D.K. Ghosh, *On NextNearestNeighbor Interaction in Linear Chain. I*, J. Math. Phys. **10**, 1388 (1969), doi:10.1063/1.1664978.

[15] C.K. Majumdar, D.K. Ghosh, *On NextNearestNeighbor Interaction in Linear Chain. II*, J. Math. Phys. **10**, 1399 (1969), doi:10.1063/1.1664979.

[16] I. Peschel, V.J. Emery, *Calculation of spin correlations in two-dimensional Ising systems from one-dimensional kinetic models*, Z. Phys. B **43**, 241 (1981), doi:10.1007/BF01297524.

[17] H. Katsura, D. Schuricht, M. Takahashi, *Exact ground states and topological order in interacting Kitaev/Majorana chains*, Phys. Rev. B **92**, 115137 (2015), doi:10.1103/PhysRevB.92.115137.

[18] P. Jordan, E. Wigner, *Über das Paulische Äquivalenzverbot*, Z. Physik **47**, 631 (1928), doi:10.1007/BF01331938.

[19] E. Sela, A. Altland, A. Rosch, *Majorana fermions in strongly interacting helical liquids*, Phys. Rev. B **84**, 085114 (2011), doi:10.1103/PhysRevB.84.085114.

[20] E. Lieb, T. Schultz, D. Mattis, *Two soluble models of an antiferromagnetic chain*, Ann. Phys. **16**, 407 (1961), doi:10.1016/0003-4916(61)90115-4.

[21] R.J. Elliott, P. Pfeuty, C. Wood, *Ising Model with a Transverse Field*, Phys. Rev. Lett. **25**, 443 (1970), doi:10.1103/PhysRevLett.25.443.

[22] P. Pfeuty, *The one-dimensional Ising model with a transverse field*, Ann. Phys. **57**, 79 (1970), doi:10.1016/0003-4916(70)90270-8.

[23] J. Kemp, N.Y. Yao, C.R. Laumann, P. Fendley, *Long coherence times for edge spins*, J. Stat. Mech. 063105 (2017), doi:10.1088/1742-5468/aa73f0.

[24] W.J. Caspers, W. Magnus, *Some exact excited states in a linear antiferromagnetic spin system*, Phys. Lett. A **88**, 103 (1982), doi:10.1016/0375-9601(82)90603-X.

[25] D.P. Arovas, *Two exact excited states for the $S = 1$ AKLT chain*, Phys. Lett. A **137**, 431 (1989), doi:10.1016/0375-9601(89)90921-3.

[26] S. Moudgalya, S. Rachel, B.A. Bernevig, N. Regnault, *Exact Excited States of Non-Integrable Models*, arXiv:1708.05021 (unpublished).

[27] A.S. Jermyn, R.S.K. Mong, J. Alicea, P. Fendley, *Stability of zero modes in parafermion chains*, Phys. Rev. B **90**, 165106 (2014), doi:10.1103/PhysRevB.90.165106.

[28] F. Iemini, C. Mora, L. Mazza, *Topological Phases of Parafermions: A Model with Exactly Solvable Ground States*, Phys. Rev. Lett. **118** 170402 (2017), doi:10.1103/PhysRevLett.118.170402.

[29] E. Fradkin, L.P. Kadanoff, *Disorder variables and parafermions in two-dimensional statistical mechanics*, Nucl. Phys. B **170** 1 (1980), doi:10.1016/0550-3213(80)90472-1.

[30] Y. Zhuang, H.J. Changlani, N.M. Tubman, T.L. Hughes, *Phase diagram of the Z_3 parafermionic chain with chiral interactions*, Phys. Rev. B **92**, 035154 (2015), doi:10.1103/PhysRevB.92.035154.

[31] N. Moran, D. Pellegrino, J.K. Slingerland, G. Kells, *Parafermionic clock models and quantum resonance*, Phys. Rev. B **95**, 235127 (2017), doi:10.1103/PhysRevB.95.235127.

[32] A.B. Zamolodchikov, V.A. Fateev, *Nonlocal (parafermion) currents in two-dimensional conformal quantum field theory and self-dual critical points in Z_N-symmetric statistical systems*, Zh. Eksp. Teor. Fiz. **89**, 380 (1985), `http://jetp.ac.ru/cgi-bin/dn/e_062_02_0215.pdf`.

[33] E. Cobanera, G. Ortiz, *Fock parafermions and self-dual representations of the braid group*, Phys. Rev. A **89** 012328 (2014), doi:10.1103/PhysRevA.89.012328.

[34] J. Kurmann, H. Thomas, G. Müller, *Antiferromagnetic long-range order in the anisotropic quantum spin chain*, Physica A **112**, 235 (1982), doi:10.1016/0378-4371(82)90217-5.

[35] D. Sen, *Large-S analysis of a quantum axial next-nearest-neighbor Ising model in one dimension*, Phys. Rev. B **43**, 5939 (1991), doi:10.1103/PhysRevB.43.5939.

[36] A. Dutta, D. sen, *Gapless line for the anisotropic Heisenberg spin−1/2 chain in a magnetic field and the quantum axial next-nearest-neighbor Ising chain*, Phys. Rev. B **67**, 094435 (2003), doi:10.1103/PhysRevB.67.094435.

[37] In the $S = 1/2$ case, the Hamiltonian Eq. (37) is $\frac{1}{4}$ times

Hamiltonian in Eq. (2), which is written in terms of Pauli operators.

[38] For $S = \frac{1}{2}$as one can see from Eq.8 there is only one such a excited state, namely e_-, since in this case $(S_1^z - S_2^z)|g_+\rangle = 0$.